Measurement of electroweak-induced production of Wγ with two jets in pp collisions at $\sqrt{s} = 8\,\text{TeV}$ and constraints on anomalous quartic gauge couplings

The CMS collaboration

E-mail: cms-publication-committee-chair@cern.ch

ABSTRACT: A measurement of electroweak-induced production of Wγ and two jets is performed, where the W boson decays leptonically. The data used in the analysis correspond to an integrated luminosity of $19.7\,\text{fb}^{-1}$ collected by the CMS experiment in $\sqrt{s} = 8\,\text{TeV}$ proton-proton collisions produced at the LHC. Candidate events are selected with exactly one muon or electron, missing transverse momentum, one photon, and two jets with large rapidity separation. An excess over the hypothesis of the standard model without electroweak production of Wγ with two jets is observed with a significance of 2.7 standard deviations. The cross section measured in the fiducial region is $10.8 \pm 4.1(\text{stat}) \pm 3.4(\text{syst}) \pm 0.3(\text{lumi})\,\text{fb}$, which is consistent with the standard model electroweak prediction. The total cross section for Wγ in association with two jets in the same fiducial region is measured to be $23.2 \pm 4.3(\text{stat}) \pm 1.7(\text{syst}) \pm 0.6(\text{lumi})\,\text{fb}$, which is consistent with the standard model prediction from the combination of electroweak- and quantum chromodynamics-induced processes. No deviations are observed from the standard model predictions and experimental limits on anomalous quartic gauge couplings $f_{M,0-7}/\Lambda^4$, $f_{T,0-2}/\Lambda^4$, and $f_{T,5-7}/\Lambda^4$ are set at 95% confidence level.

Contents

1 Introduction

In the past few decades the standard model (SM) of particle physics has achieved great success through various stringent tests and the discovery of all its predicted particles, including the recently observed Higgs boson [1–4]. Additionally, the non-Abelian nature of gauge interactions was tested by the measurements of diboson production (e.g., refs. [5–13]). The CERN LHC allows the measurement of many novel processes predicted by the SM, especially those that involve pure electroweak (EW) interactions with relatively small cross sections compared with QCD-induced production of EW final states. Typical examples include triple gauge boson production [14] and vector boson scattering (VBS) or vector boson fusion (VBF) processes [15–22].

The VBS processes have some features that can be exploited to better understand the SM in novel phase spaces and to probe new physics or constrain anomalous gauge couplings. For example, phenomenological studies of the EW production of W and Z bosons in association with two jets that exploit the large rapidity gaps between the two jets [23, 24]. Also, the VBF process was studied using the Higgs boson production and decay in refs. [25–28]. Furthermore, the EW production of Z bosons, Zγ, Zγγ, and same-sign
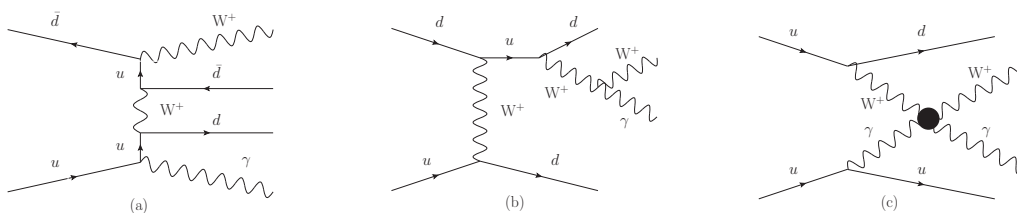
Figure 1. Representative diagrams for EW Wγ+2 jets production at the LHC corresponding to (a) bremsstrahlung, (b) bremsstrahlung with triple gauge coupling, and (c) VBS with quartic coupling.

W boson pairs in association with two jets has recently been measured at the LHC [16–18, 20, 21, 29]. Moreover, both the ATLAS and the CMS experiments found evidence for exclusive $\gamma\gamma$ to W$^+$W$^-$ production [15, 19], and the ATLAS experiment found evidence for W$\gamma\gamma$ triple boson production [30]. All the results are in good agreement with the SM predictions.

In this analysis, we search for EW-induced Wγ production in association with two jets [31] (EW Wγ+2 jets) in the W boson leptonic decay channel (W $\rightarrow \ell\nu$, $\ell =$ e, μ). This process is expected to have one of the largest cross sections of all the VBS processes and thus is expected to be one of the first VBS processes observable at a hadron collider. As shown in figure 1, Wγ production includes several different classes of diagrams: bremsstrahlung of one or two vector bosons and the more interesting VBS EW processes such as in figure 1c. The cross sections of EW-induced only and EW+QCD total Wγ processes are measured in a VBS-like fiducial region, where the two jets have a large separation in pseudorapidity. The signal structure of the weak boson scattering events makes VBS processes a good probe of quartic gauge boson couplings. Instead of measuring the SM gauge couplings, which are completely fixed by the SM SU(2)$_L \otimes$ U(1)$_Y$ gauge symmetry, we keep the SM gauge symmetry while setting limits on a set of higher dimensional anomalous quartic gauge couplings (aQGCs). More details of the aQGC parameterization can be found in appendix A.

The production of Wγ+2 jets at the LHC has two major contributions at leading order (LO) in addition to the EW signal process described above: QCD and triple gauge boson WVγ processes, with V = W or Z decaying into a quark-antiquark pair. Because these processes can have the same set of initial and final states, these three contributions interfere. One can suppress this interference by choosing an appropriate phase space for the measurements. The WVγ events reside mainly in the W or Z boson mass window; we require $m_{jj} > 200$ GeV to eliminate most of this contribution. The EW Wγ+2 jets events favor a larger m_{jj} region than the QCD Wγ+2 jets events do. Calculations using the MADGRAPH program show the interference decreases with increasing m_{jj} and $|\Delta\eta(j1, j2)|$, and can change from constructive to destructive at $\sim$1 TeV in m_{jj} depending on the choice of renormalization and factorization scales. In the analysis we consider the phase space region with $m_{jj} > 700$ GeV and $|\Delta\eta(j1, j2)| > 2.4$ to suppress the interference. The interference effect in the fiducial region is estimated to be 4.6% of the total Wγ+2 jets cross section.

In addition to the main background from QCD Wγ+2 jets production [32], other backgrounds include (1) jets misidentified as photons or electrons, (2) WVγ events with hadronically decaying V bosons (W/Z $\rightarrow jj$) and a photon from initial- or final-state radiation, (3) contributions from top quark pairs with a radiated photon, and (4) single top quark events with a radiated photon. The selection criteria are designed to reduce the collective sum of these backgrounds. In the case of nonzero anomalous couplings, the EW contribution can be greatly enhanced, especially in the high-energy tails of some kinematic distributions; therefore, we require the photon and W boson to have large transverse momenta to obtain better sensitivity.

The paper is organized as follows: section 2 describes the CMS detector. Section 3 presents the Monte Carlo event simulation and data sample and section 4 describes the event reconstruction and selection. In section 5, methods of background modeling are explained. Systematic uncertainties considered in the analysis are discussed subsequently in section 6. Results of the search for the EW signal and the measured EW and EW+QCD cross sections in the fiducial region are reported in section 7. Results on anomalous couplings using the W boson transverse momentum distribution are given in section 8. Finally, section 9 summarizes the results.

2   The CMS detector

The central feature of the CMS apparatus is a superconducting solenoid of 6 m internal diameter and 13 m length, providing a magnetic field of 3.8 T. Within the solenoid volume are a silicon pixel and strip tracker, a lead tungstate crystal electromagnetic calorimeter (ECAL), and a brass and scintillator hadron calorimeter (HCAL). Muons are reconstructed in gas-ionization detectors embedded in the steel flux-return yoke outside the solenoid. Extensive forward calorimetry complements the coverage provided by the barrel and endcap detectors.

The tracking system consists of 1440 silicon pixel and 15 148 silicon strip detector modules and covers the pseudorapidity range $|\eta| < 2.5$, providing a transverse momentum p_{T} resolution of about 1.5% at 100 GeV. The electromagnetic calorimeter consists of 75 848 lead tungstate crystals, which provide coverage in $|\eta| < 1.48$ in the barrel region (EB) and $1.48 < |\eta| < 3.00$ in the two endcap regions (EE). A preshower detector consisting of two planes of silicon sensors interleaved with three radiation lengths of lead is located in front of the EE. Photons are identified as ECAL energy clusters not linked to the extrapolation of any charged particle trajectory to the ECAL. These energy clusters are merged to form superclusters that are five crystals wide in η, centered around the most energetic crystal, and have a variable width in the azimuthal angle ϕ. The HCAL consists of a set of sampling calorimeters that utilize alternating layers of brass as absorber and plastic scintillator as active material. It provides coverage for $|\eta| < 3.0$. Combined with the forward calorimeter modules, the coverage of hadronic jets is extended to $|\eta| < 5.0$. The energy of charged hadrons is determined from a combination of the track momentum and the corresponding ECAL and HCAL energies, corrected for the combined response function of the calorimeters. The energy of neutral hadrons is obtained from the corresponding corrected ECAL and HCAL energies. The muon system includes barrel drift tubes covering

the range $|\eta| < 1.2$, endcap cathode strip chambers ($0.9 < |\eta| < 2.5$), and resistive-plate chambers ($|\eta| < 1.6$) [33]. The CMS detector is nearly hermetic, allowing for measurements of the missing transverse momentum vector $\vec{p}_{\mathrm{T}}^{\mathrm{miss}}$, which is defined as the projection on the plane perpendicular to the beams of the negative vector sum of the momenta of all reconstructed particles in an event.

The first level of the CMS trigger system, composed of custom hardware processors, uses information from the calorimeters and muon detectors to select the events of interest in a fixed time interval of less than $4\,\mu$s. The high-level trigger processor farm further decreases the event rate from around $100\,$kHz to less than $1\,$kHz, before data storage.

A more detailed description of the CMS detector, together with a definition of the coordinate system used and the relevant kinematic variables, can be found in ref. [34].

3 Data and simulated samples

The analysis uses a data sample of proton-proton collisions collected at $\sqrt{s} = 8\,$TeV by the CMS detector in 2012 that corresponds to an integrated luminosity of $19.7 \pm 0.5\,$fb^{-1} [35].

The analysis makes use of several simulated event samples based on Monte Carlo (MC). The EW W($\to \ell\nu$)γ+2 jets process and the $t\bar{t}\gamma$ background process are generated using MadGraph 5.1.3.22 [36]. Samples with aQGCs are obtained using the multi-weight method with the MadGraph 5.2.1.1 generator [37]. The MC samples for QCD W($\to \ell\nu$)/Z($\to \ell\ell$)γ+0,1,2,3 jets are also generated with the MadGraph 5.2.1.1 generator, using the MLM matching method [37–40] with a matrix element/parton shower (ME-PS) matching scale of $10\,$GeV [41]. For all samples generated with MadGraph, the CTEQ6L1 parton distribution function (PDF) set [42] is used, and the renormalization and factorization scales are set to $\sqrt{M_{\mathrm{W/Z}}^2 + (p_{\mathrm{T}}^{\mathrm{W/Z}})^2 + (p_{\mathrm{T}}^{\gamma})^2 + \sum (p_{\mathrm{T}}^j)^2}$. The single top quark production processes are generated with the POWHEG (v1.0, r1380) [43, 44] generator, using the CTEQ6M PDF set [42, 45]. The diboson samples (WW, WZ, ZZ), with one of the bosons decaying leptonically and the other decaying hadronically, are generated with PYTHIA 6.422 [46] and the CTEQ6L1 PDF set. The final-state leptons considered are e, μ, and τ, where the τ lepton decay is handled with TAUOLA [47]. The PYTHIA 6.426 [46] program is used to simulate parton showers and hadronization, with the parameters of the underlying event set to the Z2* tune [48, 49].

For all MC samples, a GEANT4-based simulation [50] of the CMS detector is used and the hard-interaction collision is overlaid with a number of simulated minimum-bias collisions. The resulting events are weighted to reproduce the data distribution of the number of inelastic collisions per bunch crossing (pileup). These simulated events are reconstructed and analyzed using the same algorithms as for data. The differences in lepton and photon reconstruction and identification (ID) efficiencies observed between data and simulated events are subsequently corrected with scale factors [51, 52].

To improve the precision of the predicted cross section for the signal model, the NLO QCD correction is included with the EW signal process through an NLO/LO cross section K factor of 1.02, determined by using VBFNLO [31, 32, 53–55]. For QCD Wγ+2 jets production, the K factor is 0.93 and is only applied for the measurement of the EW+QCD cross section, fixing the ratio between EW and QCD components.

4 Event reconstruction and selection

An EW-induced $W\gamma+2$ jets event is expected to have exactly one lepton (muon or electron), a photon, two jets with large rapidity separation, and large $|\vec{p}_T^{\text{miss}}|$.

A complete reconstruction of the individual particles emerging from each collision event is obtained via a particle-flow (PF) technique, which uses the information from all CMS subdetectors to identify and reconstruct individual particles [56, 57]. The particles are classified into mutually exclusive categories: charged hadrons, neutral hadrons, photons, muons, and electrons.

The events are selected by using single-lepton triggers with p_T thresholds of 24 GeV for muons and 27 GeV for electrons. The overall trigger efficiency is 90% (94%) for the electron (muon) data, with a small dependence on p_T and η. Charged-particle tracks are required to originate from the event primary vertex, defined as the reconstructed vertex within 24 cm (2 cm) of the center of the detector in the direction along (perpendicular to) the beam axis that has the highest value of p_T^2 summed over the associated charged-particle tracks.

The events are also required to have either one muon or one electron; events with additional charged leptons are excluded. The muon candidates are reconstructed with information from both the silicon tracker and from the muon detector by means of a global fit [33]. They are required to satisfy a requirement on the PF-based relative isolation, which is defined as the ratio of the p_T sum of all other PF candidates reconstructed in a cone $\Delta R = \sqrt{(\Delta\eta)^2 + (\Delta\phi)^2} = 0.3$ (0.4) around the candidate electron (muon) to the p_T of the candidate, and is corrected for contributions from pileup [51]. The selection efficiency is approximately 96%. Muons with $p_T > 25$ GeV and $|\eta| < 2.1$ are included in the analysis. The electron candidates are reconstructed by associating a charged particle track originating from the event primary vertex with superclusters of energy depositions in ECAL [51]. They must also satisfy the PF-based relative isolation be smaller than 0.15. The ID and isolation selection efficiency is approximately 80%. The electron candidates are further required to satisfy $p_T > 30$ GeV and $|\eta| < 2.5$, excluding the transition region between the ECAL barrel and endcaps, $1.44 < |\eta| < 1.57$, because the reconstruction of electrons in this region has lower efficiency. To suppress the $Z \to e^+e^-$ background in the electron channel, where one electron is misidentified as a photon, a Z boson mass veto of $|m_{e\gamma} - M_Z| > 10$ GeV is applied.

A well-identified and isolated photon is also required for the event selection [52]. Photons are reconstructed from superclusters and are required to satisfy a number of criteria aimed at rejecting misidentified jets. They have to have a small ratio of hadronic energy in the HCAL that is matched in (η, ϕ) to the electromagnetic energy in the ECAL; small shower shape variable $\sigma_{\eta\eta}$, which quantifies the lateral extension of the shower along the η direction [51]; small PF-based charged and neutral photon isolations including pileup corrections [56]; and an electron-track veto to reduce electron misidentification. With these requirements the photon ID and isolation efficiency is about 70%. The resulting photon candidates are further required to satisfy $p_T^\gamma > 22$ GeV and must be in the barrel region with $|\eta_{\text{sc}}| < 1.44$, where η_{sc} refers to the supercluster η, corresponding to a fiducial region in the ECAL barrel excluding the outer barrel ECAL rings of crystals.

Single-lepton (e, μ) trigger	$\lvert M_{e\gamma} - M_Z \rvert > 10\,\mathrm{GeV}$ (electron channel)
Lepton, photon ID and isolation	$p_T^{j1} > 40\,\mathrm{GeV}$, $p_T^{j2} > 30\,\mathrm{GeV}$
Second lepton veto	$\lvert \eta^{j1} \rvert < 4.7$, $\lvert \eta^{j2} \rvert < 4.7$
Muon (electron) $p_T > 25\,(30)\,\mathrm{GeV}$, $\lvert \eta \rvert < 2.1\,(2.4)$	$\lvert \Delta\phi_{j1,\vec{p}_T^{\mathrm{miss}}} \rvert > 0.4$, $\lvert \Delta\phi_{j2,\vec{p}_T^{\mathrm{miss}}} \rvert > 0.4\,\mathrm{rad}$
Photon $p_T^{\gamma} > 22\,\mathrm{GeV}$, $\lvert \eta \rvert < 1.44$	b quark jet veto for tag jets
W boson transverse mass $> 30\,\mathrm{GeV}$	Dijet invariant mass $m_{jj} > 200\,\mathrm{GeV}$
$\lvert \vec{p}_T^{\mathrm{miss}} \rvert > 35\,\mathrm{GeV}$	ΔR_{jj}, $\Delta R_{j\gamma}$, $\Delta R_{j\ell}$, $\Delta R_{\ell\gamma} > 0.5$

Table 1. Summary of the baseline selection criteria.

Jets are reconstructed from PF particles [56, 57] using the anti-k_T clustering algorithm [58] with a distance parameter of 0.5. Only charged particles with tracks originating from the primary vertex are considered for clustering. Jets from pileup are identified and removed with a pileup jet identification algorithm [59], based on both vertex information and jet shape information. Jets are required to satisfy a set of loose ID criteria designed to eliminate jets originating from noisy channels in the calorimeter [60]. Pileup collisions and the underlying event can contribute to the energy of the reconstructed jets. A correction based on the projected area of a jet on the front face of the calorimeter is used to subtract the extra energy deposited in the jet coming from pileup [61, 62]. Furthermore, the energy response in η and p_T is corrected, and the energy resolution is smeared for simulated samples to give the same response as observed [63]. An event is selected if it has at least two jets, with the leading jet $p_T > 40\,\mathrm{GeV}$, second-leading jet $p_T > 30\,\mathrm{GeV}$, and each jet within $\lvert \eta \rvert < 4.7$. These two jets are denoted as "tag jets". To suppress the WVγ background, m_{jj} is required to be at least $200\,\mathrm{GeV}$.

In addition, the event should have $\lvert \vec{p}_T^{\mathrm{miss}} \rvert > 35\,\mathrm{GeV}$. The reconstructed transverse mass of the leptonically decaying W boson, defined as $M_T = \sqrt{2p_T^{\ell} \lvert \vec{p}_T^{\mathrm{miss}} \rvert [1 - \cos(\Delta\phi_{\ell,\vec{p}_T^{\mathrm{miss}}})]}$, where $\Delta\phi_{\ell,\vec{p}_T^{\mathrm{miss}}}$ is the azimuthal angle between the lepton momentum and the $\vec{p}_T^{\mathrm{miss}}$, is required to exceed $30\,\mathrm{GeV}$ [64]. We reconstruct the leptonic W boson decay by solving for the longitudinal component of the neutrino momentum and using the mass of the W boson as a constraint. In the case of complex solutions in this reconstruction, we choose the real part of the solution, and if there are two real solutions, we choose the solution that gives a neutrino momentum vector that is closer to the longitudinal component of the corresponding charged lepton momentum.

Mismeasurement of jet energies can generate $\lvert \vec{p}_T^{\mathrm{miss}} \rvert$. To eliminate events in which this mismeasurement may generate an apparent large $\lvert \vec{p}_T^{\mathrm{miss}} \rvert$, the azimuthal separation between each of the tag jets and the $\vec{p}_T^{\mathrm{miss}}$ is required to be larger than $0.4\,\mathrm{rad}$. Additionally, to suppress the top quark backgrounds, we require that the tag jets fail a b tagging requirement of the combined secondary vertex algorithm [65] with a misidentification rate of 1%.

Separation between pairs of objects in the event is required: ΔR_{jj}, $\Delta R_{j\gamma}$, $\Delta R_{j\ell}$, and $\Delta R_{\ell\gamma} > 0.5$. All the requirements described above ensure the quality of the identified final states and comprise the baseline selections for the analysis. Table 1 summarizes these criteria.

To optimize the measurement of the EW-induced $W\gamma+2$ jets signal and improve the EW signal significance, we further consider selections on the following variables to suppress backgrounds: the Zeppenfeld variable [23], $|y_{W\gamma} - (y_{j1} + y_{j2})/2|$, calculated using the rapidities (y) of the $W\gamma$ system and the two jets; the azimuthal separation between the $W\gamma$ system, which combines the four momenta of the W boson and the photon, and the dijet system $|\Delta\phi_{W\gamma,jj}|$; the dijet invariant mass m_{jj}; and the pseudorapidity separation between the tag jets $|\Delta\eta(j1,j2)|$. These additional requirements are chosen as follows:

- $|y_{W\gamma} - (y_{j1} + y_{j2})/2| < 0.6$;

- $|\Delta\phi_{W\gamma,jj}| > 2.6\,\mathrm{rad}$;

- $m_{jj} > 700\,\mathrm{GeV}$;

- $|\Delta\eta(j1,j2)| > 2.4$.

5   Background estimation

The dominant background comes from QCD $W\gamma+$jets production. It is estimated using simulation and is normalized to the number of events in data in the region $200 < m_{jj} < 400\,\mathrm{GeV}$. The data/simulation normalization factors 0.77 ± 0.05 (muon channel) and 0.77 ± 0.06 (electron channel) are consistent with the K factor of 0.93 ± 0.27 obtained with VBFNLO. For the combined measurement of the EW+QCD cross section, the contribution of QCD $W\gamma+$jets is taken directly from simulation (scaled by the K factor) since this contribution is then no longer a background.

The background from misidentified photons arises mainly from $W+$jets events where one jet satisfies the photon ID criteria. The estimation is based on events similar to the ones selected with the baseline selection described in section 4, except that the photon must fail the tight photon ID and satisfy a looser ID requirement. This selection ensures that the photon arises from a jet, but still has kinematic properties similar to a genuine photon originating from the primary vertex. The selected events are then normalized to the number of events satisfying the tight photon ID and weighted with the probability of a jet to be misidentified as a photon. The misidentification probability is calculated as a function of photon p_T in a manner similar to that described in ref. [66]. The method uses the shapes of the $\sigma_{\eta\eta}$ and PF charged isolation distributions, which differ for genuine and misidentified photons. The fraction of the total background in the signal region contributed by this source decreases with p_T^γ, from a maximum of 33% ($p_T \approx 22\,\mathrm{GeV}$) to 6% ($p_T > 135\,\mathrm{GeV}$).

The $\gamma+$jets events contribute to the background when the jet is misidentified as a muon or electron. The contribution is found to be negligible in the muon channel, but can be significant in the electron channel, especially in the low-m_{jj} region. A control data sample is selected, in a similar way to that discussed in the previous paragraph, from the PF relative isolation sideband with a very loose electron ID requirement. Events in this control sample are then normalized to the events with signal selection and weighted with the misidentification probability for a jet to satisfy the electron selections. This probability is determined from a three-component fit to the $|\vec{p}_T^{\,\mathrm{miss}}|$ distribution considering the $\gamma+$jets

misidentified events, QCD Wγ+jets events, and misidentified photon events, as explained in more detail in ref. [64]. The γ+jets background contribution in electron channel is estimated to be 7% of the total yield for the baseline selections and negligible in the EW signal region.

Other background contributions are small and are estimated from simulation. The contributions from top quark pair and single top quark production, each in association with a photon, are suppressed with the b quark veto and represents only 3.4% of the total event yield in the EW signal region. The $Z(\to \ell\ell)\gamma(+$jets) events can contribute if one of the decayed leptons is undetected, resulting in $|\vec{p}_T^{\text{miss}}|$. The predicted cross sections of the $Z\gamma$ and WV processes decrease with increasing m_{jj} and contribute about 2% of the total SM prediction in the EW signal region.

Figure 2 shows three m_{jj} distributions in orthogonal, but signal-like, regions obtained by inverting each of three signal selection criteria: $|\Delta\eta(j1, j2)| < 2.4$; $|y_{W\gamma} - (y_{j1}+y_{j2})/2| > 0.6$; and $|\Delta\phi_{W\gamma,jj}| < 2.6$ rad. Each of these regions is enriched in QCD production of Wγ+jets events and, to a lesser degree, background having a jet misidentified as a photon. They confirm our modeling of those backgrounds.

6 Systematic uncertainties

The background rate of QCD Wγ+jets production is measured in the low-m_{jj} control region and extrapolated to the signal region. The rate uncertainty includes the statistical uncertainty as well as the uncertainties due to the misidentification probability of jets as photons or leptons. This uncertainty is 6.2% (7.1%) for the muon (electron) channel. In addition, when extrapolating from the control region to the signal region, the shape dependence on theoretical parameters affects the normalization of the QCD Wγ+jets distribution at high m_{jj}. This extrapolation uncertainty is calculated by using different MC samples with matching and renormalization/factorization scales varied up and down by a factor of two. Contributions of all the shapes are normalized in the control region and the largest absolute difference from the nominal one in the signal region is considered as the uncertainty, this is about 20% for $m_{jj} \approx 1\,\text{TeV}$.

The uncertainty on the misidentification probability of jets as electrons is estimated by considering both the $|\vec{p}_T^{\text{miss}}|$ fit uncertainty and shape uncertainty and is estimated to be 40%. There are three contributions to the uncertainties in the misidentified photon background: the statistical uncertainty, the variation in the choice of the charged isolation sideband, and the $\sigma_{\eta\eta}$ shape in the sample of events with objects misidentified as photons. The combined uncertainty, calculated in p_T^γ bins, increases from 13% at $p_T^\gamma \approx 25\,\text{GeV}$ to 54% for $p_T^\gamma \approx 135\,\text{GeV}$.

The uncertainty in the measured value of the integrated luminosity is 2.6% [35]. Jet energy scale and resolution uncertainties contribute via selection thresholds for the jet p_T and m_{jj}. We consider the uncertainties in different intervals of m_{jj}, giving a combined uncertainty varying from 12 to 31% with increasing m_{jj} in the signal region. A small difference in $|\vec{p}_T^{\text{miss}}|$ resolution [67] between data and simulation affects the signal selection efficiency by less than 1%. The uncertainties due to the lepton trigger efficiency and
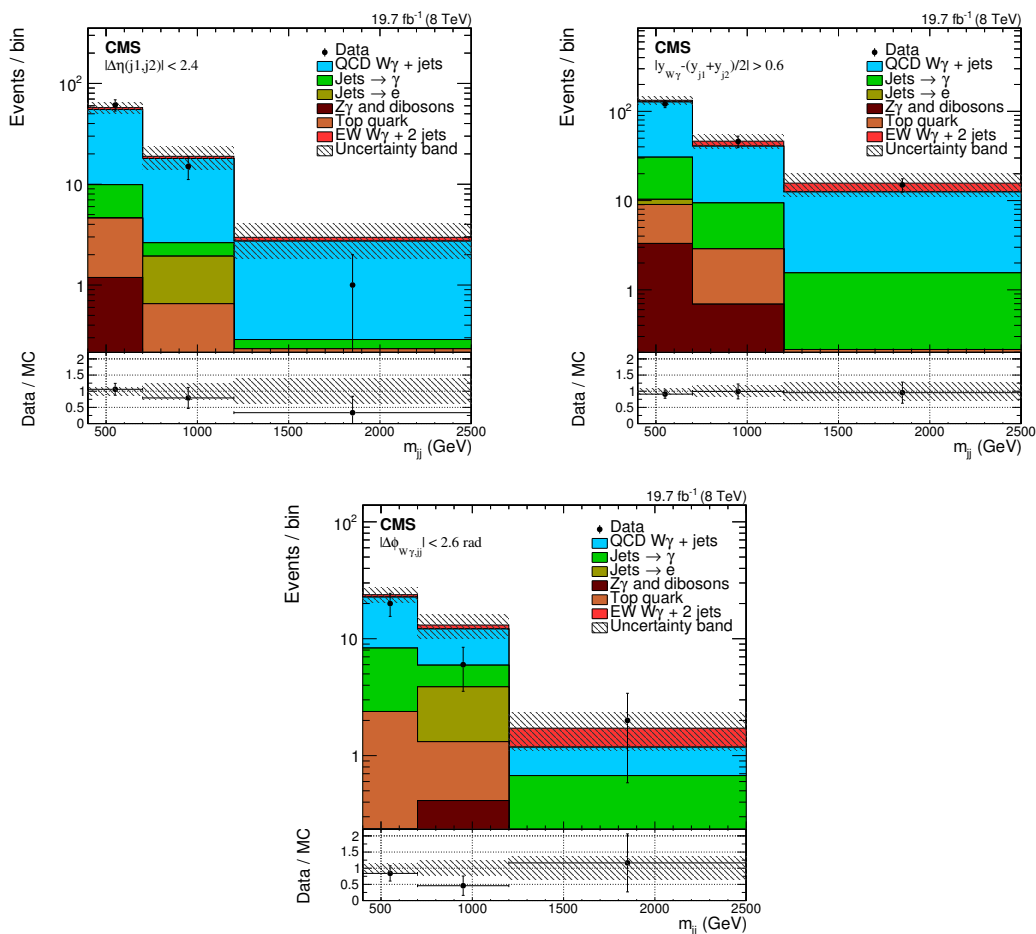
Figure 2. The m_{jj} distributions in orthogonal, but signal-like, regions obtained by inverting the signal selection criteria: $|\Delta\eta(j1, j2)| < 2.4$; $|y_{\mathrm{W}\gamma} - (y_{j1} + y_{j2})/2| > 0.6$; and $|\Delta\phi_{\mathrm{W}\gamma,jj}| < 2.6\,\mathrm{rad}$. Events from electron and muon channels are combined. Backgrounds from jets misidentified as photons (Jets $\to \gamma$) and jets misidentified as electrons (Jets $\to$ e) are estimated from data as described in the text. The diboson contribution includes $\mathrm{WV}(+\gamma)$ and $\mathrm{Z}\gamma(+\mathrm{jets})$ processes. The top quark contribution includes both the $\mathrm{t\bar{t}}\gamma$ and single top quark processes. The signal contribution is shown on top of the backgrounds. The last bin includes the overflow events. The shaded area represents the total uncertainty in the simulation, including statistical and systematic effects.

reconstruction and the selection efficiencies are estimated to be 1% and 2%, respectively. Photon reconstruction efficiency and energy scale uncertainties contribute to the signal selection efficiency at the 1% level. The uncertainty from the b jet veto procedure is 2% in the data/simulation efficiency correction factor [65]. This uncertainty has an effect of 8% on the $\mathrm{t\bar{t}}\gamma$ background, 23% on the single top quark background, and a negligible effect on the signal. The theoretical uncertainty in the $\mathrm{t\bar{t}}\gamma$ and $\mathrm{Z}\gamma$+jets production cross section is 20% [14].

The theoretical uncertainty is evaluated with VBFNLO by varying the renormalization and factorization scales, each by factors of 1/2 and 2 with the requirement that the two scales remain equal. The envelope of all the variations is taken as the uncertainty. The
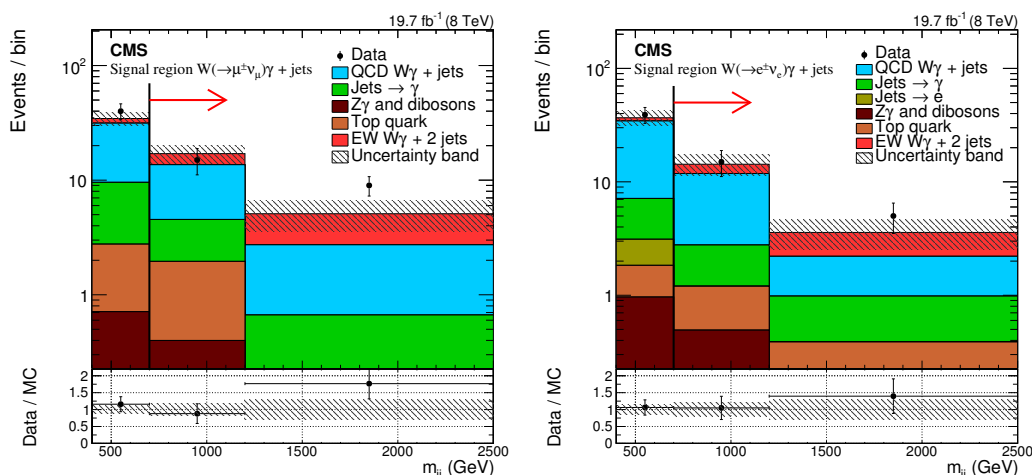
Figure 3. The m_{jj} distribution in the muon (left) and electron (right) channels, in which the signal region lies above 700 GeV, indicated by the horizontal thick arrows. Backgrounds from jets misidentified as photons (Jets $\to \gamma$) and jets misidentified as electrons (Jets $\to$ e) are estimated from data as described in the text. The diboson contribution includes WV($+\gamma$) and Zγ($+$jets) processes. The top quark contribution includes both the t$\bar{\text{t}}\gamma$ and single top quark processes. The signal contribution is shown on top of the backgrounds. The last bin includes the overflow events. The shaded area represents the total uncertainty in the simulation, including statistical and systematic effects.

uncertainty related to the PDF is calculated using the CTEQ6.1 [68] PDF uncertainty sets, following the prescription of ref. [68]. For EW Wγ+2 jets and possible aQGC signal yield, this uncertainty is found to be 20% with scale variations and 2.8% with PDF sets. For QCD Wγ+2 jets, this is 29% with scale variations and 4.2% with PDF sets. The theoretical uncertainties due to scale and PDF choices affect the expected m_{jj} shape and introduce an uncertainty in the cross section measured by fitting the m_{jj} distribution. In addition, they affect the signal and the selection acceptance and efficiency. Extrapolation from the selected region to the fiducial cross section region, defined in section 7, introduces an uncertainty of 1% in the measured fiducial cross section.

7 EW Wγ+2 jets signal and cross section measurements

A search for the SM EW Wγ+2 jets signal is performed based on the binned m_{jj} distribution, as shown in figure 3, for both the muon and electron channels, using only the two rightmost bins corresponding to $m_{jj} > 700$ GeV. The EW- and QCD-induced Wγ+2 jets production is modeled at LO, neglecting interference, with NLO QCD corrections to the cross section applied through their K factors.

We search for an enhancement in the rate of Wγ+2 jets production due to EW-induced production, treating non-Wγ and QCD-induced Wγ+2 jets production as background. The expected signal and background yields after the selections are shown in table 2.

The measured yield of data events is well described by the theoretical predictions, which include the EW contribution. A CL$_s$ based method [69–71] is used to estimate the upper limit on the EW signal strength μ_{sig}, which is defined as the ratio of the measured to

Process	Muon channel	Electron channel
EW-induced Wγ+2 jets	5.8 ± 1.8	3.8 ± 1.2
QCD-induced Wγ+jets	11.2 ± 3.2	10.3 ± 3.2
W+jets, 1 jet $\to \gamma$	3.1 ± 0.7	2.2 ± 0.5
MC t$\bar{\text{t}}\gamma$	1.2 ± 0.6	0.4 ± 0.2
MC single top quark	0.5 ± 0.5	0.6 ± 0.4
MC WVγ, V$\to$ two jets	0.3 ± 0.2	0.3 ± 0.2
MC Zγ+jets	0.2 ± 0.2	0.3 ± 0.2
Total prediction	22.1 ± 3.8	17.9 ± 3.5
Data	24	20

Table 2. Number of events for each process, with combined statistical and systematic uncertainties. The total prediction represents the sum of all the individual contributions. The W+jets background, with one jet misidentified as an electron, is negligible in the signal region.

the expected signal yield. Combining four m_{jj} bins from the two decay channels gives an upper limit of 4.3 times the SM EW prediction at a 95% confidence level (CL), compared to an expected limit of 2.0 from the background-only hypothesis.

The measured signal strength can be translated into the fiducial cross section σ_{fid} using the generated cross sections of the simulated samples σ_{gen} and an acceptance ϵ_{acc} for the total cross section from the fiducial region to the signal region: $\sigma_{\text{fid}} = \sigma_{\text{gen}}\mu_{\text{sig}}\epsilon_{\text{acc}}$. The fiducial cross section is reported in a region defined as follows:

- $p_{\text{T}}^{j1} > 30\,\text{GeV}$, $|\eta^{j1}| < 4.7$;

- $p_{\text{T}}^{j2} > 30\,\text{GeV}$, $|\eta^{j2}| < 4.7$;

- $m_{jj} > 700\,\text{GeV}$, $|\Delta\eta(j,j)| > 2.4$;

- $p_{\text{T}}^{\ell} > 20\,\text{GeV}$, $|\eta^{\ell}| < 2.4$;

- $p_{\text{T}}^{\gamma} > 20\,\text{GeV}$, $|\eta^{\gamma}| < 1.4442$;

- $|\vec{p}_{\text{T}}^{\text{miss}}| > 20\,\text{GeV}$;

- $\Delta R_{jj}, \Delta R_{\ell j}, \Delta R_{\gamma j}, \Delta R_{\ell\gamma} > 0.4$.

This phase space corresponds to the acceptance of the CMS detector, with a minimal number of additional selections on m_{jj} and $|\Delta\eta(j,j)|$ to ensure that the VBS contribution is large. It does not include requirements on the Zeppenfeld variable and the $|\Delta\phi_{\text{W}\gamma,jj}|$ variable, which are applied at the reconstruction level. The acceptance corrections for these selections are 0.289 ± 0.001 for the EW cross section and 0.174 ± 0.002 for the QCD one, where we include both PDF and scale uncertainties.

The measured cross sections and signal strengths are summarized in table 3, and the measured results are in good agreement with the theoretical predictions. The EW

Items	EW measurement	EW+QCD measurement
Signal strength $\hat{\mu}_{\text{sig}}$	$1.78^{+0.99}_{-0.76}$	$0.99^{+0.21}_{-0.19}$
Observed (expected) significance	2.7 (1.5) standard deviations	7.7 (7.5) standard deviations
Theoretical cross section (fb)	6.1 ± 1.2 (scale) ± 0.2 (PDF)	23.5 ± 5.3 (scale) ± 0.8 (PDF)
Measured cross section (fb)	10.8 ± 4.1 (stat) ± 3.4 (syst) ± 0.3 (lumi)	23.2 ± 4.3 (stat) ± 1.7 (syst) ± 0.6 (lumi)

Table 3. Summary of the measured and predicted observables.

signal strength is measured to be $\hat{\mu}_{\text{sig}} = 1.78^{+0.99}_{-0.76}$. Considering both the EW and QCD contributions as a signal, the signal strength is measured to be $0.99^{+0.21}_{-0.19}$. The EW fraction is found to be 27.1% in the search region and 25.8% in the fiducial region. The significances for both cases are also determined: for the EW signal, the observed (expected) significance is found to be 2.7 (1.5) standard deviations; for the EW+QCD signal, it is found to be 7.7 (7.5) standard deviations. The measured cross section in the fiducial region is 10.8 ± 4.1 (stat) ± 3.4 (syst) ± 0.3 (lumi) fb for the EW-induced $W\gamma+2$ jets production and 23.2 ± 4.3 (stat) ± 1.7 (syst) ± 0.6 (lumi) fb for the total $W\gamma+2$ jets production.

8 Limits on anomalous quartic gauge couplings

Following ref. [72], we parameterize the aQGCs in a formalism that maintains $SU(2)_L \otimes U(1)_Y$ gauge symmetry and leads to 14 possible dimension-eight operators that contribute to the signal. The $\mathcal{L}_{M,5}$ operator is found to be non-Hermitian and needs to be replaced by a summation of the original and its Hermitian conjugate (see appendix A for the definition). The presence of aQGCs should lead to an enhancement of the EW $W\gamma+2$ jets cross section, which should become more pronounced at the high-energy tails of some distributions. As shown in figure 4, the p_T^W distribution is sensitive to the aQGCs and therefore is used to set limits. We choose a p_T^W distribution binned over the range 50–250 GeV, with the overflow contribution included in the last bin. The shape of the distribution at high p_T^W is used to extract aQGC limits. These limits are not sensitive to small variations in the number of bins or range used for the p_T^W distribution. The events are selected with the baseline selections from section 4, with the following additional requirements: $|y_{W\gamma} - (y_{j1} + y_{j2})/2| < 1.2$, $|\Delta\eta(j1, j2)| > 2.4$, and $p_T^\gamma > 200$ GeV. A tight p_T^γ selection is applied to reach higher expected significance for the possible aQGC signal in the EW $W\gamma+2$ jets process.

The stringent selections above lead to increased statistical uncertainties in the estimations of the backgrounds. The second largest uncertainty comes from the scale variations in the predicted aQGC signal. Other uncertainties include the signal PDF choice, integrated luminosity, trigger efficiency, and lepton and photon efficiencies.

The search is performed for each aQGC parameter separately, while setting all other parameters to their SM values. Each signal sample, representing a different aQGC prediction, is generated at LO using the reweight method in MADGRAPH [37]. For each aQGC case, we compute the aQGC/SM event yield ratios for all p_T^W bins from this sample and use these ratios to rescale the SM signal shape to the enhanced aQGC shape. Then we
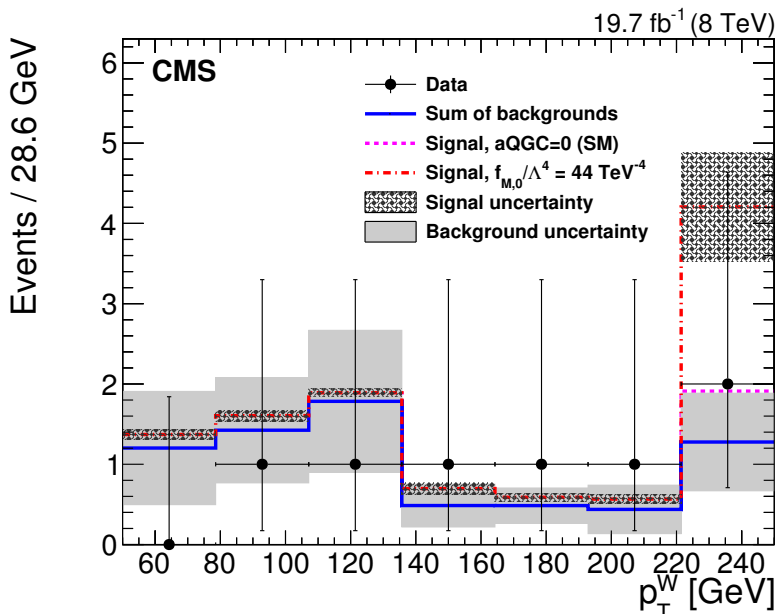
Figure 4. Comparison of predicted and observed p_T^W distributions with the combined electron and muon channels. The last p_T^W bin has been extended to include the overflow contribution. The dash-dotted line depicts a representative signal distribution with anomalous coupling parameter $f_{M,0}/\Lambda^4 = 44 \, \text{TeV}^{-4}$ and the dashed line shows the same distribution corresponding to the SM case. The bands represent the statistical and systematic uncertainties in signal and background predictions summed in quadrature. The data are shown with statistical uncertainties only.

consider the following test statistic:

$$t_\alpha = -2 \ln \frac{\mathcal{L}(\alpha, \hat{\hat{\boldsymbol{\theta}}})}{\mathcal{L}(\hat{\alpha}, \hat{\boldsymbol{\theta}})}, \qquad (8.1)$$

where the likelihood function is constructed in two lepton channels and then combined for the calculation. The α term represents the aQGC point being tested, and $\boldsymbol{\theta}$ the nuisance parameters. The $\hat{\hat{\boldsymbol{\theta}}}$ nuisance parameters correspond to the maximum of the likelihood at the point α, while $\hat{\alpha}$ and $\hat{\boldsymbol{\theta}}$ correspond to the global maximum of the likelihood. This test statistic is assumed to follow a χ^2 distribution [73, 74]. One can therefore extract the limits directly by using the delta log-likelihood function $\Delta \text{NLL} = t_\alpha/2$ [75]. Table 4 lists 95% CL exclusion limits for all parameters.

Because of the nonrenormalizable nature of higher-dimensional operators, any nonzero aQGC parameter violates unitarity at high energies. An effective theory is therefore only valid at low energies, and we need to check that the energy scale we probe is less than a new physics scale and does not violate unitarity. Sometimes a form factor is introduced to unitarize the high-energy contribution within that energy range; however, the form factor complicates the limit-setting procedure and makes it difficult to compare results among experiments. We use VBFNLO without any form factors to calculate the unitarity bound corresponding to the maximum aQGC enhancements, which would conserve unitarity within the range of energies probed at the 8 TeV LHC [53, 76]. We find that unitarity

Observed limits (TeV^{-4})	Expected limits (TeV^{-4})
$-77 < f_{M,0}/\Lambda^4 < 74$	$-47 < f_{M,0}/\Lambda^4 < 44$
$-125 < f_{M,1}/\Lambda^4 < 129$	$-72 < f_{M,1}/\Lambda^4 < 79$
$-26 < f_{M,2}/\Lambda^4 < 26$	$-16 < f_{M,2}/\Lambda^4 < 15$
$-43 < f_{M,3}/\Lambda^4 < 44$	$-25 < f_{M,3}/\Lambda^4 < 27$
$-40 < f_{M,4}/\Lambda^4 < 40$	$-23 < f_{M,4}/\Lambda^4 < 24$
$-65 < f_{M,5}/\Lambda^4 < 65$	$-39 < f_{M,5}/\Lambda^4 < 39$
$-129 < f_{M,6}/\Lambda^4 < 129$	$-77 < f_{M,6}/\Lambda^4 < 77$
$-164 < f_{M,7}/\Lambda^4 < 162$	$-99 < f_{M,7}/\Lambda^4 < 97$
$-5.4 < f_{T,0}/\Lambda^4 < 5.6$	$-3.2 < f_{T,0}/\Lambda^4 < 3.4$
$-3.7 < f_{T,1}/\Lambda^4 < 4.0$	$-2.2 < f_{T,1}/\Lambda^4 < 2.5$
$-11 < f_{T,2}/\Lambda^4 < 12$	$-6.3 < f_{T,2}/\Lambda^4 < 7.9$
$-3.8 < f_{T,5}/\Lambda^4 < 3.8$	$-2.3 < f_{T,5}/\Lambda^4 < 2.4$
$-2.8 < f_{T,6}/\Lambda^4 < 3.0$	$-1.7 < f_{T,6}/\Lambda^4 < 1.9$
$-7.3 < f_{T,7}/\Lambda^4 < 7.7$	$-4.4 < f_{T,7}/\Lambda^4 < 4.7$

Table 4. Observed and expected shape-based exclusion limits for the aQGC parameters at 95% CL, without any form factors.

is violated in many cases. We compare our results, in a consistent way, with existing limits on aQGC parameters in figure 5, where the aQGC convention used in VBFNLO has been transformed to the one that is used in our analysis. Existing competitive limits include the results from WVγ production [14], same-sign WW production [17], exclusive $\gamma\gamma \to$ WW production at the ATLAS and the CMS experiments [15, 19, 77], and W$\gamma\gamma$ production at the ATLAS experiment [30]. The limits on the a_0^W/Λ^2 and a_C^W/Λ^2 couplings in these references are transformed to ours by using eq. (2) in ref. [14], with the constraint of $f_{M,0}/\Lambda^4 = 2f_{M,2}/\Lambda^4$ and $f_{M,1}/\Lambda^4 = 2f_{M,3}/\Lambda^4$. All of the aQGC limits shown are calculated without a form factor.

9 Summary

A search for EW-induced Wγ+2 jets production and aQGCs has been presented based on events containing a W boson that decays to a lepton and a neutrino, a hard photon, and two jets with large pseudorapidity separation. The data analyzed correspond to an integrated luminosity of 19.7 fb^{-1} collected in proton-proton collisions at $\sqrt{s} = 8$ TeV with the CMS detector at the LHC. An excess is observed above the expectation from QCD-induced Wγ+2 jets and other backgrounds, with an observed (expected) significance of 2.7 (1.5) standard deviations. The corresponding cross section within the VBS-like fiducial region is measured to be 10.8 ± 4.1 (stat) ± 3.4 (syst) ± 0.3 (lumi) fb, which is consistent with the SM prediction of EW-induced signal. In the same fiducial region, the total cross
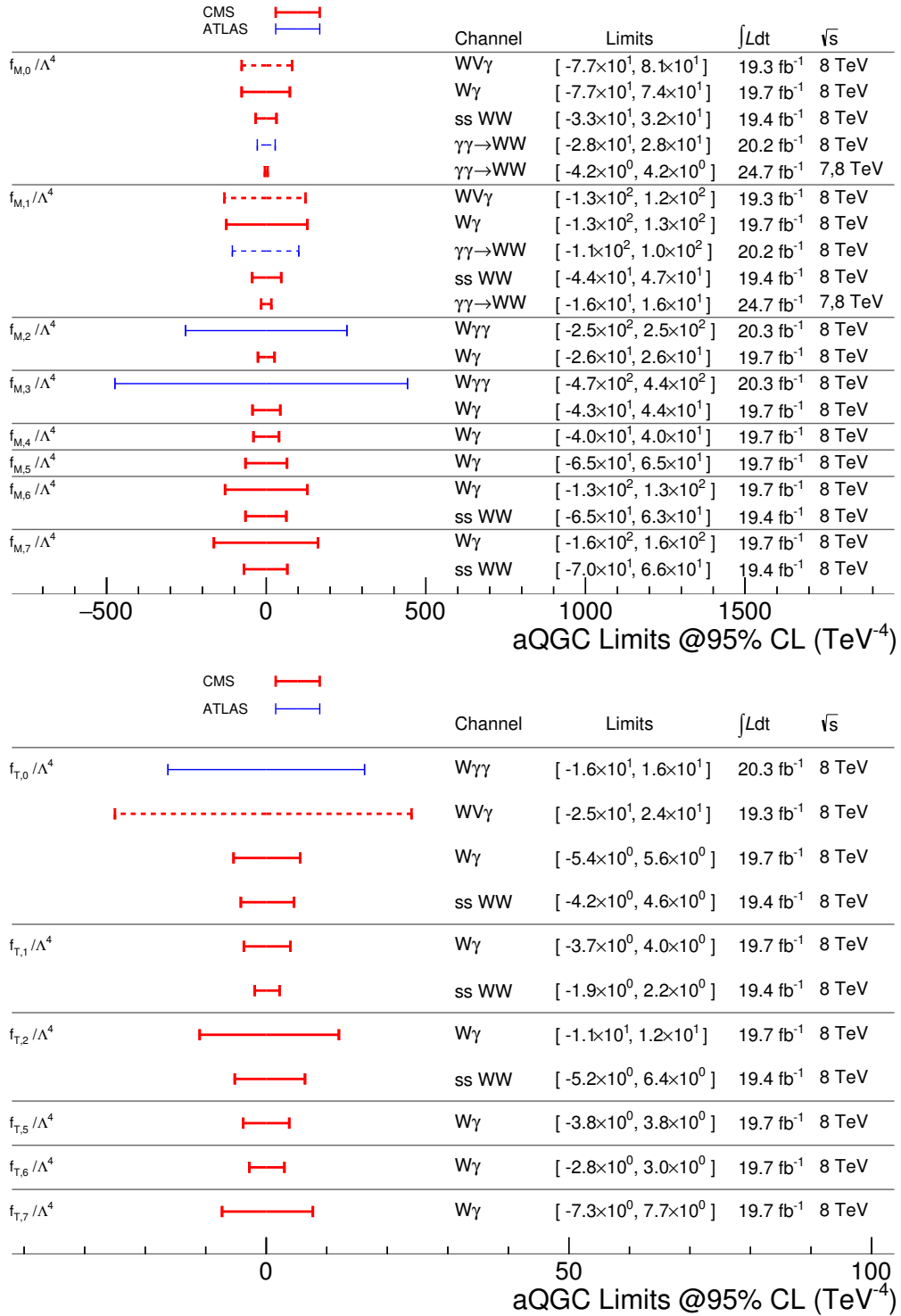
Figure 5. Comparison of the limits on the dimension-eight aQGC parameters obtained from this study Wγ, together with results from the production of WVγ [14], same-sign WW [17], exclusive γγ → WW in ATLAS and CMS [15, 19, 77], and Wγγ in ATLAS [30]. The limits from the CMS experiment are represented by thicker lines. The limits that are translated from another formalism are represented with dashed lines; details are found in ref. [14].

section for $W\gamma+2$ jets is measured to be $23.2 \pm 4.3\,(\text{stat}) \pm 1.7\,(\text{syst}) \pm 0.6\,(\text{lumi})$ fb, which is consistent with the SM EW+QCD prediction. Exclusion limits for aQGC parameters $f_{M,0-7}/\Lambda^4$, $f_{T,0-2}/\Lambda^4$, and $f_{T,5-7}/\Lambda^4$ are set at 95% CL. Competitive limits are obtained for several parameters and first limits are set on the $f_{M,4}/\Lambda^4$ and $f_{T,5-7}/\Lambda^4$ parameters.

Acknowledgments

A   Anomalous quartic gauge coupling parameterization

Gauge boson self-interactions are fixed by the gauge symmetries of the SM. To investigate possible deviations from the SM, we parameterize the aQGCs in a formalism that maintains the $SU(2)_L \otimes U(1)_Y$ gauge symmetry. As a natural extension to the SM, the lowest order pure anomalous quartic couplings arise from dimension-eight operators. This analysis

adopts the following effective Lagrangian containing such aQGCs [72]:

$$
\begin{aligned}
\mathcal{L}_{\text{aQGC}} = {} & \frac{f_{M,0}}{\Lambda^4}\,\mathrm{Tr}\,[\mathbf{W}_{\mu\nu}\mathbf{W}^{\mu\nu}] \times \left[(D_\beta\Phi)^\dagger D^\beta\Phi\right] + \frac{f_{M,1}}{\Lambda^4}\,\mathrm{Tr}\left[\mathbf{W}_{\mu\nu}\mathbf{W}^{\nu\beta}\right]\times\left[(D_\beta\Phi)^\dagger D^\mu\Phi\right] \\
& + \frac{f_{M,2}}{\Lambda^4}\,[B_{\mu\nu}B^{\mu\nu}]\times\left[(D_\beta\Phi)^\dagger D^\beta\Phi\right] + \frac{f_{M,3}}{\Lambda^4}\,\left[B_{\mu\nu}B^{\nu\beta}\right]\times\left[(D_\beta\Phi)^\dagger D^\mu\Phi\right] \\
& + \frac{f_{M,4}}{\Lambda^4}\,\left[(D_\mu\Phi)^\dagger\mathbf{W}_{\beta\nu}D^\mu\Phi\right]\times B^{\beta\nu} \\
& + \frac{f_{M,5}}{\Lambda^4}\,\times\frac{1}{2}\left[(D_\mu\Phi)^\dagger\mathbf{W}_{\beta\nu}D^\nu\Phi + (D^\nu\Phi)^\dagger\mathbf{W}_{\beta\nu}D_\mu\Phi\right]\times B^{\beta\mu} \\
& + \frac{f_{M,6}}{\Lambda^4}\,\left[(D_\mu\Phi)^\dagger\mathbf{W}_{\beta\nu}\mathbf{W}^{\beta\nu}D^\mu\Phi\right] + \frac{f_{M,7}}{\Lambda^4}\,\left[(D_\mu\Phi)^\dagger\mathbf{W}_{\beta\nu}\mathbf{W}^{\beta\mu}D^\nu\Phi\right] \\
& + \frac{f_{T,0}}{\Lambda^4}Tr[\mathbf{W}_{\mu\nu}\mathbf{W}^{\mu\nu}]\times Tr[\mathbf{W}_{\alpha\beta}\mathbf{W}^{\alpha\beta}] + \frac{f_{T,1}}{\Lambda^4}Tr[\mathbf{W}_{\alpha\nu}\mathbf{W}^{\mu\beta}]\times Tr[\mathbf{W}_{\mu\beta}\mathbf{W}^{\alpha\nu}] \\
& + \frac{f_{T,2}}{\Lambda^4}Tr[\mathbf{W}_{\alpha\mu}\mathbf{W}^{\mu\beta}]\times Tr[\mathbf{W}_{\beta\nu}\mathbf{W}^{\nu\alpha}] + \frac{f_{T,5}}{\Lambda^4}Tr[\mathbf{W}_{\mu\nu}\mathbf{W}^{\mu\nu}]\times B_{\alpha\beta}B^{\alpha\beta} \\
& + \frac{f_{T,6}}{\Lambda^4}Tr[\mathbf{W}_{\alpha\nu}\mathbf{W}^{\mu\beta}]\times B_{\mu\beta}B^{\alpha\nu} + \frac{f_{T,7}}{\Lambda^4}Tr[\mathbf{W}_{\alpha\mu}\mathbf{W}^{\mu\beta}]\times B_{\beta\nu}B^{\nu\alpha},
\end{aligned}
\tag{A.1}
$$

where Φ represents the Higgs doublet, $B_{\mu\nu}$ and $W^i_{\mu\nu}$ are the associated field strength tensors of the U(1)$_Y$ and SU(2)$_L$ gauge symmetries, and $\mathbf{W}_{\mu\nu} \equiv \sum_j W^j_{\mu\nu}\sigma^j/2$. The f_T/Λ^4 associated operators characterize the effect of new physics on the scattering of transversely polarized vector bosons, and f_M/Λ^4 includes mixed transverse and longitudinal scatterings; however, pure longitudinal scattering effects do not occur in the Wγ final state due to the presence of the photon. The listed operators include all contributions to the WW$\gamma\gamma$ and WWZγ vertices. In this paper, we set $c = 1$ to describe energy, momentum, and mass in units of GeV.

Any nonzero value in aQGCs will lead to tree-level unitarity violation at sufficiently high energy and could be unitarized with a suitable form factor; however the unitarization depends on the detailed structure of new physics, which is not known a priori. Following ref. [14], the choice is made to set limits without using a form factor.

References

[1] ATLAS collaboration, *Observation of a new particle in the search for the Standard Model Higgs boson with the ATLAS detector at the LHC*, *Phys. Lett.* **B 716** (2012) 1 [arXiv:1207.7214] [INSPIRE].

[2] CMS collaboration, *Observation of a new boson at a mass of 125 GeV with the CMS experiment at the LHC*, *Phys. Lett.* **B 716** (2012) 30 [arXiv:1207.7235] [INSPIRE].

[3] CMS collaboration, *Observation of a new boson with mass near 125 GeV in pp collisions at $\sqrt{s} = 7$ and 8 TeV*, *JHEP* **06** (2013) 081 [arXiv:1303.4571] [INSPIRE].

[4] ATLAS and CMS collaborations, *Combined measurement of the Higgs boson mass in pp collisions at $\sqrt{s} = 7$ and 8 TeV with the ATLAS and CMS experiments*, *Phys. Rev. Lett.* **114** (2015) 191803 [arXiv:1503.07589] [INSPIRE].

[5] CMS collaboration, *Measurement of the $pp \to ZZ$ production cross section and constraints on anomalous triple gauge couplings in four-lepton final states at $\sqrt{s} = 8$ TeV*, *Phys. Lett.* **B 740** (2015) 250 [arXiv:1406.0113] [INSPIRE].

[6] CMS collaboration, *Measurement of W^+W^- and ZZ production cross sections in pp collisions at $\sqrt{s} = 8$ TeV*, *Phys. Lett.* **B 721** (2013) 190 [arXiv:1301.4698] [INSPIRE].

[7] CMS collaboration, *Measurement of the sum of WW and WZ production with $W+$ dijet events in pp collisions at $\sqrt{s} = 7$ TeV*, *Eur. Phys. J.* **C 73** (2013) 2283 [arXiv:1210.7544] [INSPIRE].

[8] ATLAS collaboration, *Measurement of W^+W^- production in pp collisions at $\sqrt{s} = 7$ TeV with the ATLAS detector and limits on anomalous WWZ and $WW\gamma$ couplings*, *Phys. Rev.* **D 87** (2013) 112001 [arXiv:1210.2979] [INSPIRE].

[9] CMS collaboration, *Measurements of the Z Z production cross sections in the 2l2ν channel in proton–proton collisions at $\sqrt{s} = 7$ and 8 TeV and combined constraints on triple gauge couplings*, *Eur. Phys. J.* **C 75** (2015) 511 [arXiv:1503.05467] [INSPIRE].

[10] CMS collaboration, *Measurement of the W^+W^- cross section in pp collisions at $\sqrt{s} = 8$ TeV and limits on anomalous gauge couplings*, *Eur. Phys. J.* **C 76** (2016) 401 [arXiv:1507.03268] [INSPIRE].

[11] ATLAS collaboration, *Measurement of WZ production in proton-proton collisions at $\sqrt{s} = 7$ TeV with the ATLAS detector*, *Eur. Phys. J.* **C 72** (2012) 2173 [arXiv:1208.1390] [INSPIRE].

[12] CMS collaboration, *Measurement of the $W\gamma$ and $Z\gamma$ inclusive cross sections in pp collisions at $\sqrt{s} = 7$ TeV and limits on anomalous triple gauge boson couplings*, *Phys. Rev.* **D 89** (2014) 092005 [arXiv:1308.6832] [INSPIRE].

[13] ATLAS collaboration, *Measurements of $W\gamma$ and $Z\gamma$ production in pp collisions at $\sqrt{s} = 7$ TeV with the ATLAS detector at the LHC*, *Phys. Rev.* **D 87** (2013) 112003 [arXiv:1302.1283] [INSPIRE].

[14] CMS collaboration, *Search for $WW\gamma$ and $WZ\gamma$ production and constraints on anomalous quartic gauge couplings in pp collisions at $\sqrt{s} = 8$ TeV*, *Phys. Rev.* **D 90** (2014) 032008 [arXiv:1404.4619] [INSPIRE].

[15] ATLAS collaboration, *Measurement of exclusive $\gamma\gamma \to W^+W^-$ production and search for exclusive Higgs boson production in pp collisions at $\sqrt{s} = 8$ TeV using the ATLAS detector*, *Phys. Rev.* **D 94** (2016) 032011 [arXiv:1607.03745] [INSPIRE].

[16] ATLAS collaboration, *Evidence for electroweak production of $W^\pm W^\pm jj$ in pp collisions at $\sqrt{s} = 8$ TeV with the ATLAS detector*, *Phys. Rev. Lett.* **113** (2014) 141803 [arXiv:1405.6241] [INSPIRE].

[17] CMS collaboration, *Study of vector boson scattering and search for new physics in events with two same-sign leptons and two jets*, *Phys. Rev. Lett.* **114** (2015) 051801 [arXiv:1410.6315] [INSPIRE].

[18] CMS collaboration, *Measurement of the hadronic activity in events with a Z and two jets and extraction of the cross section for the electroweak production of a Z with two jets in pp collisions at $\sqrt{s} = 7$ TeV*, *JHEP* **10** (2013) 062 [arXiv:1305.7389] [ɪɴSPIRE].

[19] CMS collaboration, *Evidence for exclusive $\gamma\gamma \to W^+W^-$ production and constraints on anomalous quartic gauge couplings in pp collisions at $\sqrt{s} = 7$ and 8 TeV*, *JHEP* **08** (2016) 119 [arXiv:1604.04464] [ɪɴSPIRE].

[20] ATLAS collaboration, *Measurement of the electroweak production of dijets in association with a Z-boson and distributions sensitive to vector boson fusion in proton-proton collisions at $\sqrt{s} = 8$ TeV using the ATLAS detector*, *JHEP* **04** (2014) 031 [arXiv:1401.7610] [ɪɴSPIRE].

[21] CMS collaboration, *Measurement of electroweak production of two jets in association with a Z boson in proton-proton collisions at $\sqrt{s} = 8$ TeV*, *Eur. Phys. J.* **C 75** (2015) 66 [arXiv:1410.3153] [ɪɴSPIRE].

[22] CMS collaboration, *Measurement of electroweak production of a W boson and two forward jets in proton-proton collisions at $\sqrt{s} = 8$ TeV*, *JHEP* **11** (2016) 147 [arXiv:1607.06975] [ɪɴSPIRE].

[23] D.L. Rainwater, R. Szalapski and D. Zeppenfeld, *Probing color singlet exchange in Z + two jet events at the CERN LHC*, *Phys. Rev.* **D 54** (1996) 6680 [hep-ph/9605444] [ɪɴSPIRE].

[24] V.A. Khoze, M.G. Ryskin, W.J. Stirling and P.H. Williams, *A Z monitor to calibrate Higgs production via vector boson fusion with rapidity gaps at the LHC*, *Eur. Phys. J.* **C 26** (2003) 429 [hep-ph/0207365] [ɪɴSPIRE].

[25] D.L. Rainwater, D. Zeppenfeld and K. Hagiwara, *Searching for $H \to \tau^+\tau^-$ in weak boson fusion at the CERN LHC*, *Phys. Rev.* **D 59** (1998) 014037 [hep-ph/9808468] [ɪɴSPIRE].

[26] T. Plehn, D.L. Rainwater and D. Zeppenfeld, *A Method for identifying $H \to \tau^+\tau^- \to e^\pm \mu^\mp p_T$ at the CERN LHC*, *Phys. Rev.* **D 61** (2000) 093005 [hep-ph/9911385] [ɪɴSPIRE].

[27] D.L. Rainwater and D. Zeppenfeld, *Observing $H \to W^*W^* \to e^\pm \mu^\mp \not{p}_T$ in weak boson fusion with dual forward jet tagging at the CERN LHC*, *Phys. Rev.* **D 60** (1999) 113004 [*Erratum ibid.* **D 61** (2000) 099901] [hep-ph/9906218] [ɪɴSPIRE].

[28] N. Kauer, T. Plehn, D.L. Rainwater and D. Zeppenfeld, *$H \to W^+W^-$ as the discovery mode for a light Higgs boson*, *Phys. Lett.* **B 503** (2001) 113 [hep-ph/0012351] [ɪɴSPIRE].

[29] ATLAS collaboration, *Measurements of $Z\gamma$ and $Z\gamma\gamma$ production in pp collisions at $\sqrt{s} = 8$ TeV with the ATLAS detector*, *Phys. Rev.* **D 93** (2016) 112002 [arXiv:1604.05232] [ɪɴSPIRE].

[30] ATLAS collaboration, *Evidence of $W\gamma\gamma$ production in pp collisions at $\sqrt{s} = 8$ TeV and limits on anomalous quartic gauge couplings with the ATLAS detector*, *Phys. Rev. Lett.* **115** (2015) 031802 [arXiv:1503.03243] [ɪɴSPIRE].

[31] F. Campanario, N. Kaiser and D. Zeppenfeld, *$W\gamma$ production in vector boson fusion at NLO in QCD*, *Phys. Rev.* **D 89** (2014) 014009 [arXiv:1309.7259] [ɪɴSPIRE].

[32] F. Campanario, M. Kerner, L.D. Ninh and D. Zeppenfeld, *Next-to-leading order QCD corrections to $W\gamma$ production in association with two jets*, *Eur. Phys. J.* **C 74** (2014) 2882 [arXiv:1402.0505] [ɪɴSPIRE].

[33] CMS collaboration, *Performance of CMS muon reconstruction in pp collision events at* $\sqrt{s} = 7$ *TeV*, 2012 *JINST* **7** P10002 [`arXiv:1206.4071`] [ɪɴSPIRE].

[34] CMS collaboration, *The CMS experiment at the CERN LHC*, 2008 *JINST* **3** S08004 [ɪɴSPIRE].

[35] CMS collaboration, *CMS luminosity based on pixel cluster counting — Summer 2013 update*, CMS-PAS-LUM-13-001 (2013).

[36] J. Alwall, M. Herquet, F. Maltoni, O. Mattelaer and T. Stelzer, *MadGraph* 5*: going beyond*, *JHEP* **06** (2011) 128 [`arXiv:1106.0522`] [ɪɴSPIRE].

[37] J. Alwall et al., *The automated computation of tree-level and next-to-leading order differential cross sections and their matching to parton shower simulations*, *JHEP* **07** (2014) 079 [`arXiv:1405.0301`] [ɪɴSPIRE].

[38] S. Catani, F. Krauss, R. Kuhn and B.R. Webber, *QCD matrix elements + parton showers*, *JHEP* **11** (2001) 063 [`hep-ph/0109231`] [ɪɴSPIRE].

[39] J. Alwall, S. de Visscher and F. Maltoni, *QCD radiation in the production of heavy colored particles at the LHC*, *JHEP* **02** (2009) 017 [`arXiv:0810.5350`] [ɪɴSPIRE].

[40] J. Alwall et al., *Comparative study of various algorithms for the merging of parton showers and matrix elements in hadronic collisions*, *Eur. Phys. J.* **C 53** (2008) 473 [`arXiv:0706.2569`] [ɪɴSPIRE].

[41] S. Hoeche et al., *Matching parton showers and matrix elements*, in the proceedings of *HERA and the LHC: Workshop on the implications of HERA for LHC physics*, March 24–27, CERN, Switzerland (2006), `hep-ph/0602031` [ɪɴSPIRE].

[42] J. Pumplin, D.R. Stump, J. Huston, H.L. Lai, P.M. Nadolsky and W.K. Tung, *New generation of parton distributions with uncertainties from global QCD analysis*, *JHEP* **07** (2002) 012 [`hep-ph/0201195`] [ɪɴSPIRE].

[43] S. Alioli, P. Nason, C. Oleari and E. Re, *NLO single-top production matched with shower in POWHEG: s- and t-channel contributions*, *JHEP* **09** (2009) 111 [*Erratum ibid.* **02** (2010) 011] [`arXiv:0907.4076`] [ɪɴSPIRE].

[44] E. Re, *Single-top Wt-channel production matched with parton showers using the POWHEG method*, *Eur. Phys. J.* **C 71** (2011) 1547 [`arXiv:1009.2450`] [ɪɴSPIRE].

[45] P.M. Nadolsky et al., *Implications of CTEQ global analysis for collider observables*, *Phys. Rev.* **D 78** (2008) 013004 [`arXiv:0802.0007`] [ɪɴSPIRE].

[46] T. Sjöstrand, S. Mrenna and P.Z. Skands, *PYTHIA 6.4 physics and manual*, *JHEP* **05** (2006) 026 [`hep-ph/0603175`] [ɪɴSPIRE].

[47] S. Jadach, J.H. Kuhn and Z. Was, *TAUOLA : a library of Monte Carlo programs to simulate decays of polarized τ leptons*, CERN-TH-5856-90 (1990).

[48] CMS collaboration, *Measurement of the underlying event activity at the LHC with* $\sqrt{s} = 7$ *TeV and comparison with* $\sqrt{s} = 0.9$ *TeV*, *JHEP* **09** (2011) 109 [`arXiv:1107.0330`] [ɪɴSPIRE].

[49] CMS collaboration, *Study of the underlying event at forward rapidity in pp collisions at* $\sqrt{s} = 0.9$, 2.76 *and* 7 *TeV*, *JHEP* **04** (2013) 072 [`arXiv:1302.2394`] [ɪɴSPIRE].

[50] GEANT4 collaboration, S. Agostinelli et al., *GEANT4 — a simulation toolkit*, *Nucl. Instrum. Meth.* **A 506** (2003) 250 [ɪɴSPIRE].

[51] CMS collaboration, *Performance of electron reconstruction and selection with the CMS detector in proton-proton collisions at $\sqrt{s} = 8$ TeV*, 2015 *JINST* **10** P06005 [arXiv:1502.02701] [INSPIRE].

[52] CMS collaboration, *Performance of photon reconstruction and identification with the CMS detector in proton-proton collisions at $\sqrt{s} = 8$ TeV*, 2015 *JINST* **10** P08010 [arXiv:1502.02702] [INSPIRE].

[53] J. Baglio et al., *Release note — VBFNLO 2.7.0*, arXiv:1404.3940 [INSPIRE].

[54] K. Arnold et al., *VBFNLO: a parton level Monte Carlo for processes with electroweak bosons — Manual for version 2.5.0*, arXiv:1107.4038 [INSPIRE].

[55] K. Arnold et al., *VBFNLO: a parton level Monte Carlo for processes with electroweak bosons*, *Comput. Phys. Commun.* **180** (2009) 1661 [arXiv:0811.4559] [INSPIRE].

[56] CMS collaboration, *Particle-flow event reconstruction in CMS and performance for jets, taus and MET*, CMS-PAS-PFT-09-001 (2009).

[57] CMS collaboration, *Commissioning of the particle-flow event reconstruction with the first LHC collisions recorded in the CMS detector*, CMS-PAS-PFT-10-001 (2010).

[58] M. Cacciari, G.P. Salam and G. Soyez, *The anti-k_t jet clustering algorithm*, *JHEP* **04** (2008) 063 [arXiv:0802.1189] [INSPIRE].

[59] CMS collaboration, *Pileup jet identification*, CMS-PAS-JME-13-005 (2013).

[60] CMS collaboration, *Identification and filtering of uncharacteristic noise in the CMS hadron calorimeter*, 2010 *JINST* **5** T03014 [arXiv:0911.4881] [INSPIRE].

[61] M. Cacciari and G.P. Salam, *Pileup subtraction using jet areas*, *Phys. Lett.* **B 659** (2008) 119 [arXiv:0707.1378] [INSPIRE].

[62] M. Cacciari, G.P. Salam and G. Soyez, *The catchment area of jets*, *JHEP* **04** (2008) 005 [arXiv:0802.1188] [INSPIRE].

[63] CMS collaboration, *Determination of jet energy calibration and transverse momentum resolution in CMS*, 2011 *JINST* **6** P11002 [arXiv:1107.4277] [INSPIRE].

[64] CMS collaboration, *Measurement of the inclusive W and Z production cross sections in pp collisions at $\sqrt{s} = 7$ TeV*, *JHEP* **10** (2011) 132 [arXiv:1107.4789] [INSPIRE].

[65] CMS collaboration, *Identification of b-quark jets with the CMS experiment*, 2013 *JINST* **8** P04013 [arXiv:1211.4462] [INSPIRE].

[66] CMS collaboration, *Measurement of $W\gamma$ and $Z\gamma$ production in pp collisions at $\sqrt{s} = 7$ TeV*, *Phys. Lett.* **B 701** (2011) 535 [arXiv:1105.2758] [INSPIRE].

[67] CMS collaboration, *Missing transverse energy performance of the CMS detector*, 2011 *JINST* **6** P09001 [arXiv:1106.5048] [INSPIRE].

[68] D. Stump et al., *Inclusive jet production, parton distributions and the search for new physics*, *JHEP* **10** (2003) 046 [hep-ph/0303013] [INSPIRE].

[69] ATLAS collaboration, *Procedure for the LHC Higgs boson search combination in summer 2011*, ATL-PHYS-PUB-2011-011 (2011).

[70] A.L. Read, *Presentation of search results: the CL_s technique*, *J. Phys.* **C 28** (2002) 2693

[71] T. Junk, *Confidence level computation for combining searches with small statistics*, *Nucl. Instrum. Meth.* **A 434** (1999) 435 [hep-ex/9902006] [INSPIRE].

[72] O.J.P. Eboli, M.C. Gonzalez-Garcia and J.K. Mizukoshi, $pp \to jje^{\pm}\mu^{\pm}\nu\nu$ and $jje^{\pm}mu^{\mp}\nu\nu$ at $O(\alpha_{em}^6)$ and $O(\alpha_{em}^4\alpha_s^2)$ for the study of the quartic electroweak gauge boson vertex at CERN LHC, *Phys. Rev.* **D 74** (2006) 073005 [hep-ph/0606118] [INSPIRE].

[73] A. Wald, *Tests of statistical hypotheses concerning several parameters when the number of observations is large*, *Trans. Amer. Math. Soc.* **54** (1943) 426.

[74] S.S. Wilks, *The large-sample distribution of the likelihood ratio for testing composite hypotheses*, *Ann. Math. Statist.* **9** (1938) 60,

[75] CMS collaboration, *Precise determination of the mass of the Higgs boson and tests of compatibility of its couplings with the standard model predictions using proton collisions at* 7 *and* 8 *TeV*, *Eur. Phys. J.* **C 75** (2015) 212 [arXiv:1412.8662] [INSPIRE].

[76] G.J. Gounaris, J. Layssac and F.M. Renard, *Unitarity constraints for transverse gauge bosons at LEP and supercolliders*, *Phys. Lett.* **B 332** (1994) 146 [hep-ph/9311370] [INSPIRE].

[77] CMS collaboration, *Study of exclusive two-photon production of* W^+W^- *in pp collisions at* $\sqrt{s} = 7$ *TeV and constraints on anomalous quartic gauge couplings*, *JHEP* **07** (2013) 116 [arXiv:1305.5596] [INSPIRE].

The CMS collaboration

Yerevan Physics Institute, Yerevan, Armenia

V. Khachatryan, A.M. Sirunyan, A. Tumasyan

Institut für Hochenergiephysik, Wien, Austria

W. Adam, E. Asilar, T. Bergauer, J. Brandstetter, E. Brondolin, M. Dragicevic, J. Erö, M. Flechl, M. Friedl, R. Frühwirth[1], V.M. Ghete, C. Hartl, N. Hörmann, J. Hrubec, M. Jeitler[1], A. König, I. Krätschmer, D. Liko, T. Matsushita, I. Mikulec, D. Rabady, N. Rad, B. Rahbaran, H. Rohringer, J. Schieck[1], J. Strauss, W. Treberer-Treberspurg, W. Waltenberger, C.-E. Wulz[1]

National Centre for Particle and High Energy Physics, Minsk, Belarus

V. Mossolov, N. Shumeiko, J. Suarez Gonzalez

Universiteit Antwerpen, Antwerpen, Belgium

S. Alderweireldt, E.A. De Wolf, X. Janssen, J. Lauwers, M. Van De Klundert, H. Van Haevermaet, P. Van Mechelen, N. Van Remortel, A. Van Spilbeeck

Vrije Universiteit Brussel, Brussel, Belgium

S. Abu Zeid, F. Blekman, J. D'Hondt, N. Daci, I. De Bruyn, K. Deroover, N. Heracleous, S. Lowette, S. Moortgat, L. Moreels, A. Olbrechts, Q. Python, S. Tavernier, W. Van Doninck, P. Van Mulders, I. Van Parijs

Université Libre de Bruxelles, Bruxelles, Belgium

H. Brun, C. Caillol, B. Clerbaux, G. De Lentdecker, H. Delannoy, G. Fasanella, L. Favart, R. Goldouzian, A. Grebenyuk, G. Karapostoli, T. Lenzi, A. Léonard, J. Luetic, T. Maerschalk, A. Marinov, A. Randle-conde, T. Seva, C. Vander Velde, P. Vanlaer, R. Yonamine, F. Zenoni, F. Zhang[2]

Ghent University, Ghent, Belgium

A. Cimmino, T. Cornelis, D. Dobur, A. Fagot, G. Garcia, M. Gul, D. Poyraz, S. Salva, R. Schöfbeck, M. Tytgat, W. Van Driessche, E. Yazgan, N. Zaganidis

Université Catholique de Louvain, Louvain-la-Neuve, Belgium

H. Bakhshiansohi, C. Beluffi[3], O. Bondu, S. Brochet, G. Bruno, A. Caudron, S. De Visscher, C. Delaere, M. Delcourt, B. Francois, A. Giammanco, A. Jafari, P. Jez, M. Komm, V. Lemaitre, A. Magitteri, A. Mertens, M. Musich, C. Nuttens, K. Piotrzkowski, L. Quertenmont, M. Selvaggi, M. Vidal Marono, S. Wertz

Université de Mons, Mons, Belgium

N. Beliy

Centro Brasileiro de Pesquisas Fisicas, Rio de Janeiro, Brazil

W.L. Aldá Júnior, F.L. Alves, G.A. Alves, L. Brito, C. Hensel, A. Moraes, M.E. Pol, P. Rebello Teles

Universidade do Estado do Rio de Janeiro, Rio de Janeiro, Brazil

E. Belchior Batista Das Chagas, W. Carvalho, J. Chinellato[4], A. Custódio, E.M. Da Costa, G.G. Da Silveira[5], D. De Jesus Damiao, C. De Oliveira Martins, S. Fonseca De Souza, L.M. Huertas Guativa, H. Malbouisson, D. Matos Figueiredo, C. Mora Herrera, L. Mundim, H. Nogima, W.L. Prado Da Silva, A. Santoro, A. Sznajder, E.J. Tonelli Manganote[4], A. Vilela Pereira

Universidade Estadual Paulista [a], **Universidade Federal do ABC** [b], **São Paulo, Brazil**

S. Ahuja[a], C.A. Bernardes[b], S. Dogra[a], T.R. Fernandez Perez Tomei[a], E.M. Gregores[b], P.G. Mercadante[b], C.S. Moon[a], S.F. Novaes[a], Sandra S. Padula[a], D. Romero Abad[b], J.C. Ruiz Vargas

Institute for Nuclear Research and Nuclear Energy, Sofia, Bulgaria

A. Aleksandrov, R. Hadjiiska, P. Iaydjiev, M. Rodozov, S. Stoykova, G. Sultanov, M. Vutova

University of Sofia, Sofia, Bulgaria

A. Dimitrov, I. Glushkov, L. Litov, B. Pavlov, P. Petkov

Beihang University, Beijing, China

W. Fang[6]

Institute of High Energy Physics, Beijing, China

M. Ahmad, J.G. Bian, G.M. Chen, H.S. Chen, M. Chen, Y. Chen[7], T. Cheng, C.H. Jiang, D. Leggat, Z. Liu, F. Romeo, S.M. Shaheen, A. Spiezia, J. Tao, C. Wang, Z. Wang, H. Zhang, J. Zhao

State Key Laboratory of Nuclear Physics and Technology, Peking University, Beijing, China

Y. Ban, G. Chen, Q. Li, S. Liu, Y. Mao, S.J. Qian, D. Wang, Z. Xu, D. Yang, Z. Zhang

Universidad de Los Andes, Bogota, Colombia

C. Avila, A. Cabrera, L.F. Chaparro Sierra, C. Florez, J.P. Gomez, C.F. González Hernández, J.D. Ruiz Alvarez, J.C. Sanabria

University of Split, Faculty of Electrical Engineering, Mechanical Engineering and Naval Architecture, Split, Croatia

N. Godinovic, D. Lelas, I. Puljak, P.M. Ribeiro Cipriano, T. Sculac

University of Split, Faculty of Science, Split, Croatia

Z. Antunovic, M. Kovac

Institute Rudjer Boskovic, Zagreb, Croatia

V. Brigljevic, D. Ferencek, K. Kadija, S. Micanovic, L. Sudic, T. Susa

University of Cyprus, Nicosia, Cyprus

A. Attikis, G. Mavromanolakis, J. Mousa, C. Nicolaou, F. Ptochos, P.A. Razis, H. Rykaczewski

Charles University, Prague, Czech Republic

M. Finger[8], M. Finger Jr.[8]

Universidad San Francisco de Quito, Quito, Ecuador

E. Carrera Jarrin

Academy of Scientific Research and Technology of the Arab Republic of Egypt, Egyptian Network of High Energy Physics, Cairo, Egypt

A.A. Abdelalim[9,10], Y. Mohammed[11], E. Salama[12,13]

National Institute of Chemical Physics and Biophysics, Tallinn, Estonia

B. Calpas, M. Kadastik, M. Murumaa, L. Perrini, M. Raidal, A. Tiko, C. Veelken

Department of Physics, University of Helsinki, Helsinki, Finland

P. Eerola, J. Pekkanen, M. Voutilainen

Helsinki Institute of Physics, Helsinki, Finland

J. Härkönen, V. Karimäki, R. Kinnunen, T. Lampén, K. Lassila-Perini, S. Lehti, T. Lindén, P. Luukka, T. Peltola, J. Tuominiemi, E. Tuovinen, L. Wendland

Lappeenranta University of Technology, Lappeenranta, Finland

J. Talvitie, T. Tuuva

IRFU, CEA, Université Paris-Saclay, Gif-sur-Yvette, France

M. Besancon, F. Couderc, M. Dejardin, D. Denegri, B. Fabbro, J.L. Faure, C. Favaro, F. Ferri, S. Ganjour, S. Ghosh, A. Givernaud, P. Gras, G. Hamel de Monchenault, P. Jarry, I. Kucher, E. Locci, M. Machet, J. Malcles, J. Rander, A. Rosowsky, M. Titov, A. Zghiche

Laboratoire Leprince-Ringuet, Ecole Polytechnique, IN2P3-CNRS, Palaiseau, France

A. Abdulsalam, I. Antropov, S. Baffioni, F. Beaudette, P. Busson, L. Cadamuro, E. Chapon, C. Charlot, O. Davignon, R. Granier de Cassagnac, M. Jo, S. Lisniak, P. Miné, M. Nguyen, C. Ochando, G. Ortona, P. Paganini, P. Pigard, S. Regnard, R. Salerno, Y. Sirois, T. Strebler, Y. Yilmaz, A. Zabi

Institut Pluridisciplinaire Hubert Curien (IPHC), Université de Strasbourg, CNRS-IN2P3

J.-L. Agram[14], J. Andrea, A. Aubin, D. Bloch, J.-M. Brom, M. Buttignol, E.C. Chabert, N. Chanon, C. Collard, E. Conte[14], X. Coubez, J.-C. Fontaine[14], D. Gelé, U. Goerlach, A.-C. Le Bihan, J.A. Merlin[15], K. Skovpen, P. Van Hove

Centre de Calcul de l'Institut National de Physique Nucleaire et de Physique des Particules, CNRS/IN2P3, Villeurbanne, France

S. Gadrat

Université de Lyon, Université Claude Bernard Lyon 1, CNRS-IN2P3, Institut de Physique Nucléaire de Lyon, Villeurbanne, France

S. Beauceron, C. Bernet, G. Boudoul, E. Bouvier, C.A. Carrillo Montoya, R. Chierici, D. Contardo, B. Courbon, P. Depasse, H. El Mamouni, J. Fan, J. Fay, S. Gascon,

M. Gouzevitch, G. Grenier, B. Ille, F. Lagarde, I.B. Laktineh, M. Lethuillier, L. Mirabito, A.L. Pequegnot, S. Perries, A. Popov[16], D. Sabes, V. Sordini, M. Vander Donckt, P. Verdier, S. Viret

Georgian Technical University, Tbilisi, Georgia

A. Khvedelidze[8]

Tbilisi State University, Tbilisi, Georgia

Z. Tsamalaidze[8]

RWTH Aachen University, I. Physikalisches Institut, Aachen, Germany

C. Autermann, S. Beranek, L. Feld, A. Heister, M.K. Kiesel, K. Klein, M. Lipinski, A. Ostapchuk, M. Preuten, F. Raupach, S. Schael, C. Schomakers, J.F. Schulte, J. Schulz, T. Verlage, H. Weber, V. Zhukov[16]

RWTH Aachen University, III. Physikalisches Institut A, Aachen, Germany

M. Brodski, E. Dietz-Laursonn, D. Duchardt, M. Endres, M. Erdmann, S. Erdweg, T. Esch, R. Fischer, A. Güth, M. Hamer, T. Hebbeker, C. Heidemann, K. Hoepfner, S. Knutzen, M. Merschmeyer, A. Meyer, P. Millet, S. Mukherjee, M. Olschewski, K. Padeken, T. Pook, M. Radziej, H. Reithler, M. Rieger, F. Scheuch, L. Sonnenschein, D. Teyssier, S. Thüer

RWTH Aachen University, III. Physikalisches Institut B, Aachen, Germany

V. Cherepanov, G. Flügge, W. Haj Ahmad, F. Hoehle, B. Kargoll, T. Kress, A. Künsken, J. Lingemann, T. Müller, A. Nehrkorn, A. Nowack, I.M. Nugent, C. Pistone, O. Pooth, A. Stahl[15]

Deutsches Elektronen-Synchrotron, Hamburg, Germany

M. Aldaya Martin, C. Asawatangtrakuldee, K. Beernaert, O. Behnke, U. Behrens, A.A. Bin Anuar, K. Borras[17], A. Campbell, P. Connor, C. Contreras-Campana, F. Costanza, C. Diez Pardos, G. Dolinska, G. Eckerlin, D. Eckstein, E. Eren, E. Gallo[18], J. Garay Garcia, A. Geiser, A. Gizhko, J.M. Grados Luyando, P. Gunnellini, A. Harb, J. Hauk, M. Hempel[19], H. Jung, A. Kalogeropoulos, O. Karacheban[19], M. Kasemann, J. Keaveney, J. Kieseler, C. Kleinwort, I. Korol, D. Krücker, W. Lange, A. Lelek, J. Leonard, K. Lipka, A. Lobanov, W. Lohmann[19], R. Mankel, I.-A. Melzer-Pellmann, A.B. Meyer, G. Mittag, J. Mnich, A. Mussgiller, E. Ntomari, D. Pitzl, R. Placakyte, A. Raspereza, B. Roland, M.Ö. Sahin, P. Saxena, T. Schoerner-Sadenius, C. Seitz, S. Spannagel, N. Stefaniuk, K.D. Trippkewitz, G.P. Van Onsem, R. Walsh, C. Wissing

University of Hamburg, Hamburg, Germany

V. Blobel, M. Centis Vignali, A.R. Draeger, T. Dreyer, E. Garutti, D. Gonzalez, J. Haller, M. Hoffmann, A. Junkes, R. Klanner, R. Kogler, N. Kovalchuk, T. Lapsien, T. Lenz, I. Marchesini, D. Marconi, M. Meyer, M. Niedziela, D. Nowatschin, F. Pantaleo[15], T. Peiffer, A. Perieanu, J. Poehlsen, C. Sander, C. Scharf, P. Schleper, A. Schmidt, S. Schumann, J. Schwandt, H. Stadie, G. Steinbrück, F.M. Stober, M. Stöver, H. Tholen, D. Troendle, E. Usai, L. Vanelderen, A. Vanhoefer, B. Vormwald

Institut für Experimentelle Kernphysik, Karlsruhe, Germany

C. Barth, C. Baus, J. Berger, E. Butz, T. Chwalek, F. Colombo, W. De Boer, A. Dierlamm, S. Fink, R. Friese, M. Giffels, A. Gilbert, P. Goldenzweig, D. Haitz, F. Hartmann[15], S.M. Heindl, U. Husemann, I. Katkov[16], P. Lobelle Pardo, B. Maier, H. Mildner, M.U. Mozer, Th. Müller, M. Plagge, G. Quast, K. Rabbertz, S. Röcker, F. Roscher, M. Schröder, I. Shvetsov, G. Sieber, H.J. Simonis, R. Ulrich, J. Wagner-Kuhr, S. Wayand, M. Weber, T. Weiler, S. Williamson, C. Wöhrmann, R. Wolf

Institute of Nuclear and Particle Physics (INPP), NCSR Demokritos, Aghia Paraskevi, Greece

G. Anagnostou, G. Daskalakis, T. Geralis, V.A. Giakoumopoulou, A. Kyriakis, D. Loukas, I. Topsis-Giotis

National and Kapodistrian University of Athens, Athens, Greece

A. Agapitos, S. Kesisoglou, A. Panagiotou, N. Saoulidou, E. Tziaferi

University of Ioánnina, Ioánnina, Greece

I. Evangelou, G. Flouris, C. Foudas, P. Kokkas, N. Loukas, N. Manthos, I. Papadopoulos, E. Paradas

MTA-ELTE Lendület CMS Particle and Nuclear Physics Group, Eötvös Loránd University, Budapest, Hungary

N. Filipovic

Wigner Research Centre for Physics, Budapest, Hungary

G. Bencze, C. Hajdu, P. Hidas, D. Horvath[20], F. Sikler, V. Veszpremi, G. Vesztergombi[21], A.J. Zsigmond

Institute of Nuclear Research ATOMKI, Debrecen, Hungary

N. Beni, S. Czellar, J. Karancsi[22], A. Makovec, J. Molnar, Z. Szillasi

Institute of Physics, University of Debrecen

M. Bartók[21], P. Raics, Z.L. Trocsanyi, B. Ujvari

National Institute of Science Education and Research, Bhubaneswar, India

S. Bahinipati, S. Choudhury[23], P. Mal, K. Mandal, A. Nayak[24], D.K. Sahoo, N. Sahoo, S.K. Swain

Panjab University, Chandigarh, India

S. Bansal, S.B. Beri, V. Bhatnagar, R. Chawla, U.Bhawandeep, A.K. Kalsi, A. Kaur, M. Kaur, R. Kumar, A. Mehta, M. Mittal, J.B. Singh, G. Walia

University of Delhi, Delhi, India

Ashok Kumar, A. Bhardwaj, B.C. Choudhary, R.B. Garg, S. Keshri, S. Malhotra, M. Naimuddin, N. Nishu, K. Ranjan, R. Sharma, V. Sharma

Saha Institute of Nuclear Physics, Kolkata, India

R. Bhattacharya, S. Bhattacharya, K. Chatterjee, S. Dey, S. Dutt, S. Dutta, S. Ghosh, N. Majumdar, A. Modak, K. Mondal, S. Mukhopadhyay, S. Nandan, A. Purohit, A. Roy, D. Roy, S. Roy Chowdhury, S. Sarkar, M. Sharan, S. Thakur

Indian Institute of Technology Madras, Madras, India

P.K. Behera

Bhabha Atomic Research Centre, Mumbai, India

R. Chudasama, D. Dutta, V. Jha, V. Kumar, A.K. Mohanty[15], P.K. Netrakanti, L.M. Pant, P. Shukla, A. Topkar

Tata Institute of Fundamental Research-A, Mumbai, India

T. Aziz, S. Dugad, G. Kole, B. Mahakud, S. Mitra, G.B. Mohanty, B. Parida, N. Sur, B. Sutar

Tata Institute of Fundamental Research-B, Mumbai, India

S. Banerjee, S. Bhowmik[25], R.K. Dewanjee, S. Ganguly, M. Guchait, Sa. Jain, S. Kumar, M. Maity[25], G. Majumder, K. Mazumdar, T. Sarkar[25], N. Wickramage[26]

Indian Institute of Science Education and Research (IISER), Pune, India

S. Chauhan, S. Dube, V. Hegde, A. Kapoor, K. Kothekar, A. Rane, S. Sharma

Institute for Research in Fundamental Sciences (IPM), Tehran, Iran

H. Behnamian, S. Chenarani[27], E. Eskandari Tadavani, S.M. Etesami[27], A. Fahim[28], M. Khakzad, M. Mohammadi Najafabadi, M. Naseri, S. Paktinat Mehdiabadi, F. Rezaei Hosseinabadi, B. Safarzadeh[29], M. Zeinali

University College Dublin, Dublin, Ireland

M. Felcini, M. Grunewald

INFN Sezione di Bari ^{a}, Università di Bari ^{b}, Politecnico di Bari ^{c}, Bari, Italy

M. Abbrescia^{a,b}, C. Calabria^{a,b}, C. Caputo^{a,b}, A. Colaleo^a, D. Creanza^{a,c}, L. Cristella^{a,b}, N. De Filippis^{a,c}, M. De Palma^{a,b}, L. Fiore^a, G. Iaselli^{a,c}, G. Maggi^{a,c}, M. Maggi^a, G. Miniello^{a,b}, S. My^{a,b}, S. Nuzzo^{a,b}, A. Pompili^{a,b}, G. Pugliese^{a,c}, R. Radogna^{a,b}, A. Ranieri^a, G. Selvaggi^{a,b}, L. Silvestris^{a,15}, R. Venditti^{a,b}, P. Verwilligen^a

INFN Sezione di Bologna ^{a}, Università di Bologna ^{b}, Bologna, Italy

G. Abbiendi^a, C. Battilana, D. Bonacorsi^{a,b}, S. Braibant-Giacomelli^{a,b}, L. Brigliadori^{a,b}, R. Campanini^{a,b}, P. Capiluppi^{a,b}, A. Castro^{a,b}, F.R. Cavallo^a, S.S. Chhibra^{a,b}, G. Codispoti^{a,b}, M. Cuffiani^{a,b}, G.M. Dallavalle^a, F. Fabbri^a, A. Fanfani^{a,b}, D. Fasanella^{a,b}, P. Giacomelli^a, C. Grandi^a, L. Guiducci^{a,b}, S. Marcellini^a, G. Masetti^a, A. Montanari^a, F.L. Navarria^{a,b}, A. Perrotta^a, A.M. Rossi^{a,b}, T. Rovelli^{a,b}, G.P. Siroli^{a,b}, N. Tosi^{a,b,15}

INFN Sezione di Catania ^{a}, Università di Catania ^{b}, Catania, Italy

S. Albergo^{a,b}, M. Chiorboli^{a,b}, S. Costa^{a,b}, A. Di Mattia^a, F. Giordano^{a,b}, R. Potenza^{a,b}, A. Tricomi^{a,b}, C. Tuve^{a,b}

INFN Sezione di Firenze ^{a}, Università di Firenze ^{b}, Firenze, Italy

G. Barbagli^a, V. Ciulli^{a,b}, C. Civinini^a, R. D'Alessandro^{a,b}, E. Focardi^{a,b}, V. Gori^{a,b}, P. Lenzi^{a,b}, M. Meschini^a, S. Paoletti^a, G. Sguazzoni^a, L. Viliani^{a,b,15}

INFN Laboratori Nazionali di Frascati, Frascati, Italy

L. Benussi, S. Bianco, F. Fabbri, D. Piccolo, F. Primavera^{15}

INFN Sezione di Genova ^{a}, Università di Genova ^{b}, Genova, Italy

V. Calvelli^{a,b}, F. Ferro^a, M. Lo Vetere^{a,b}, M.R. Monge^{a,b}, E. Robutti^a, S. Tosi^{a,b}

INFN Sezione di Milano-Bicocca ^{a}, Università di Milano-Bicocca ^{b}, Milano, Italy

L. Brianza^{15}, M.E. Dinardo^{a,b}, S. Fiorendi^{a,b}, S. Gennai^a, A. Ghezzi^{a,b}, P. Govoni^{a,b}, M. Malberti, S. Malvezzi^a, R.A. Manzoni^{a,b,15}, B. Marzocchi^{a,b}, D. Menasce^a, L. Moroni^a, M. Paganoni^{a,b}, D. Pedrini^a, S. Pigazzini, S. Ragazzi^{a,b}, T. Tabarelli de Fatis^{a,b}

INFN Sezione di Napoli ^{a}, Università di Napoli 'Federico II' ^{b}, Napoli, Italy, Università della Basilicata ^{c}, Potenza, Italy, Università G. Marconi ^{d}, Roma, Italy

S. Buontempo^a, N. Cavallo^{a,c}, G. De Nardo, S. Di Guida^{a,d,15}, M. Esposito^{a,b}, F. Fabozzi^{a,c}, A.O.M. Iorio^{a,b}, G. Lanza^a, L. Lista^a, S. Meola^{a,d,15}, P. Paolucci^{a,15}, C. Sciacca^{a,b}, F. Thyssen

INFN Sezione di Padova ^{a}, Università di Padova ^{b}, Padova, Italy, Università di Trento ^{c}, Trento, Italy

P. Azzi^{a,15}, N. Bacchetta^a, L. Benato^{a,b}, D. Bisello^{a,b}, A. Boletti^{a,b}, R. Carlin^{a,b}, A. Carvalho Antunes De Oliveira^{a,b}, P. Checchia^a, M. Dall'Osso^{a,b}, P. De Castro Manzano^a, T. Dorigo^a, U. Dosselli^a, F. Gasparini^{a,b}, U. Gasparini^{a,b}, A. Gozzelino^a, S. Lacaprara^a, M. Margoni^{a,b}, A.T. Meneguzzo^{a,b}, J. Pazzini^{a,b,15}, N. Pozzobon^{a,b}, P. Ronchese^{a,b}, F. Simonetto^{a,b}, E. Torassa^a, M. Zanetti, P. Zotto^{a,b}, A. Zucchetta^{a,b}, G. Zumerle^{a,b}

INFN Sezione di Pavia ^{a}, Università di Pavia ^{b}, Pavia, Italy

A. Braghieri^a, A. Magnani^{a,b}, P. Montagna^{a,b}, S.P. Ratti^{a,b}, V. Re^a, C. Riccardi^{a,b}, P. Salvini^a, I. Vai^{a,b}, P. Vitulo^{a,b}

INFN Sezione di Perugia ^{a}, Università di Perugia ^{b}, Perugia, Italy

L. Alunni Solestizi^{a,b}, G.M. Bilei^a, D. Ciangottini^{a,b}, L. Fanò^{a,b}, P. Lariccia^{a,b}, R. Leonardi^{a,b}, G. Mantovani^{a,b}, M. Menichelli^a, A. Saha^a, A. Santocchia^{a,b}

INFN Sezione di Pisa ^{a}, Università di Pisa ^{b}, Scuola Normale Superiore di Pisa ^{c}, Pisa, Italy

K. Androsov^{a,30}, P. Azzurri^{a,15}, G. Bagliesi^a, J. Bernardini^a, T. Boccali^a, R. Castaldi^a, M.A. Ciocci^{a,30}, R. Dell'Orso^a, S. Donato^{a,c}, G. Fedi, A. Giassi^a, M.T. Grippo^{a,30}, F. Ligabue^{a,c}, T. Lomtadze^a, L. Martini^{a,b}, A. Messineo^{a,b}, F. Palla^a, A. Rizzi^{a,b}, A. Savoy-Navarro^{a,31}, P. Spagnolo^a, R. Tenchini^a, G. Tonelli^{a,b}, A. Venturi^a, P.G. Verdini^a

INFN Sezione di Roma ^{a}, Università di Roma ^{b}, Roma, Italy

L. Barone^{a,b}, F. Cavallari^a, M. Cipriani^{a,b}, G. D'imperio^{a,b,15}, D. Del Re^{a,b,15}, M. Diemoz^a, S. Gelli^{a,b}, C. Jorda^a, E. Longo^{a,b}, F. Margaroli^{a,b}, P. Meridiani^a, G. Organtini^{a,b}, R. Paramatti^a, F. Preiato^{a,b}, S. Rahatlou^{a,b}, C. Rovelli^a, F. Santanastasio^{a,b}

INFN Sezione di Torino ^{a}, Università di Torino ^{b}, Torino, Italy, Università del Piemonte Orientale ^{c}, Novara, Italy

N. Amapane^{a,b}, R. Arcidiacono^{a,c,15}, S. Argiro^{a,b}, M. Arneodo^{a,c}, N. Bartosik^a, R. Bellan^{a,b}, C. Biino^a, N. Cartiglia^a, F. Cenna^{a,b}, M. Costa^{a,b}, R. Covarelli^{a,b}, A. Degano^{a,b}, N. Demaria^a, L. Finco^{a,b}, B. Kiani^{a,b}, C. Mariotti^a, S. Maselli^a, E. Migliore^{a,b}, V. Monaco^{a,b}, E. Monteil^{a,b}, M.M. Obertino^{a,b}, L. Pacher^{a,b}, N. Pastrone^a, M. Pelliccioni^a, G.L. Pinna Angioni^{a,b}, F. Ravera^{a,b}, A. Romero^{a,b}, M. Ruspa^{a,c}, R. Sacchi^{a,b}, K. Shchelina^{a,b}, V. Sola^a, A. Solano^{a,b}, A. Staiano^a, P. Traczyk^{a,b}

INFN Sezione di Trieste ^{a}, Università di Trieste ^{b}, Trieste, Italy

S. Belforte^a, M. Casarsa^a, F. Cossutti^a, G. Della Ricca^{a,b}, C. La Licata^{a,b}, A. Schizzi^{a,b}, A. Zanetti^a

Kyungpook National University, Daegu, Korea

D.H. Kim, G.N. Kim, M.S. Kim, S. Lee, S.W. Lee, Y.D. Oh, S. Sekmen, D.C. Son, Y.C. Yang

Chonbuk National University, Jeonju, Korea

A. Lee

Hanyang University, Seoul, Korea

J.A. Brochero Cifuentes, T.J. Kim

Korea University, Seoul, Korea

S. Cho, S. Choi, Y. Go, D. Gyun, S. Ha, B. Hong, Y. Jo, Y. Kim, B. Lee, K. Lee, K.S. Lee, S. Lee, J. Lim, S.K. Park, Y. Roh

Seoul National University, Seoul, Korea

J. Almond, J. Kim, H. Lee, S.B. Oh, B.C. Radburn-Smith, S.h. Seo, U.K. Yang, H.D. Yoo, G.B. Yu

University of Seoul, Seoul, Korea

M. Choi, H. Kim, H. Kim, J.H. Kim, J.S.H. Lee, I.C. Park, G. Ryu, M.S. Ryu

Sungkyunkwan University, Suwon, Korea

Y. Choi, J. Goh, C. Hwang, J. Lee, I. Yu

Vilnius University, Vilnius, Lithuania

V. Dudenas, A. Juodagalvis, J. Vaitkus

National Centre for Particle Physics, Universiti Malaya, Kuala Lumpur, Malaysia

I. Ahmed, Z.A. Ibrahim, J.R. Komaragiri, M.A.B. Md Ali^{32}, F. Mohamad Idris^{33}, W.A.T. Wan Abdullah, M.N. Yusli, Z. Zolkapli

Centro de Investigacion y de Estudios Avanzados del IPN, Mexico City, Mexico

H. Castilla-Valdez, E. De La Cruz-Burelo, I. Heredia-De La Cruz[34], A. Hernandez-Almada, R. Lopez-Fernandez, R. Magaña Villalba, J. Mejia Guisao, A. Sanchez-Hernandez

Universidad Iberoamericana, Mexico City, Mexico

S. Carrillo Moreno, C. Oropeza Barrera, F. Vazquez Valencia

Benemerita Universidad Autonoma de Puebla, Puebla, Mexico

S. Carpinteyro, I. Pedraza, H.A. Salazar Ibarguen, C. Uribe Estrada

Universidad Autónoma de San Luis Potosí, San Luis Potosí, Mexico

A. Morelos Pineda

University of Auckland, Auckland, New Zealand

D. Krofcheck

University of Canterbury, Christchurch, New Zealand

P.H. Butler

National Centre for Physics, Quaid-I-Azam University, Islamabad, Pakistan

A. Ahmad, M. Ahmad, Q. Hassan, H.R. Hoorani, W.A. Khan, M.A. Shah, M. Shoaib, M. Waqas

National Centre for Nuclear Research, Swierk, Poland

H. Bialkowska, M. Bluj, B. Boimska, T. Frueboes, M. Górski, M. Kazana, K. Nawrocki, K. Romanowska-Rybinska, M. Szleper, P. Zalewski

Institute of Experimental Physics, Faculty of Physics, University of Warsaw, Warsaw, Poland

K. Bunkowski, A. Byszuk[35], K. Doroba, A. Kalinowski, M. Konecki, J. Krolikowski, M. Misiura, M. Olszewski, M. Walczak

Laboratório de Instrumentação e Física Experimental de Partículas, Lisboa, Portugal

P. Bargassa, C. Beirão Da Cruz E Silva, A. Di Francesco, P. Faccioli, P.G. Ferreira Parracho, M. Gallinaro, J. Hollar, N. Leonardo, L. Lloret Iglesias, M.V. Nemallapudi, J. Rodrigues Antunes, J. Seixas, O. Toldaiev, D. Vadruccio, J. Varela, P. Vischia

Joint Institute for Nuclear Research, Dubna, Russia

P. Bunin, I. Golutvin, I. Gorbunov, V. Karjavin, V. Korenkov, A. Lanev, A. Malakhov, V. Matveev[36,37], V.V. Mitsyn, P. Moisenz, V. Palichik, V. Perelygin, S. Shmatov, S. Shulha, N. Skatchkov, V. Smirnov, E. Tikhonenko, N. Voytishin, A. Zarubin

Petersburg Nuclear Physics Institute, Gatchina (St. Petersburg), Russia

L. Chtchipounov, V. Golovtsov, Y. Ivanov, V. Kim[38], E. Kuznetsova[39], V. Murzin, V. Oreshkin, V. Sulimov, A. Vorobyev

Institute for Nuclear Research, Moscow, Russia

Yu. Andreev, A. Dermenev, S. Gninenko, N. Golubev, A. Karneyeu, M. Kirsanov, N. Krasnikov, A. Pashenkov, D. Tlisov, A. Toropin

Institute for Theoretical and Experimental Physics, Moscow, Russia

V. Epshteyn, V. Gavrilov, N. Lychkovskaya, V. Popov, I. Pozdnyakov, G. Safronov, A. Spiridonov, M. Toms, E. Vlasov, A. Zhokin

Moscow Institute of Physics and Technology, Moscow, Russia

A. Bylinkin[37]

National Research Nuclear University 'Moscow Engineering Physics Institute' (MEPhI), Moscow, Russia

M. Chadeeva[40], E. Popova, E. Tarkovskii

P.N. Lebedev Physical Institute, Moscow, Russia

V. Andreev, M. Azarkin[37], I. Dremin[37], M. Kirakosyan, A. Leonidov[37], S.V. Rusakov, A. Terkulov

Skobeltsyn Institute of Nuclear Physics, Lomonosov Moscow State University, Moscow, Russia

A. Baskakov, A. Belyaev, E. Boos, M. Dubinin[41], L. Dudko, A. Ershov, A. Gribushin, V. Klyukhin, O. Kodolova, I. Lokhtin, I. Miagkov, S. Obraztsov, S. Petrushanko, V. Savrin, A. Snigirev

Novosibirsk State University (NSU), Novosibirsk, Russia

V. Blinov[42], Y.Skovpen[42]

State Research Center of Russian Federation, Institute for High Energy Physics, Protvino, Russia

I. Azhgirey, I. Bayshev, S. Bitioukov, D. Elumakhov, V. Kachanov, A. Kalinin, D. Konstantinov, V. Krychkine, V. Petrov, R. Ryutin, A. Sobol, S. Troshin, N. Tyurin, A. Uzunian, A. Volkov

University of Belgrade, Faculty of Physics and Vinca Institute of Nuclear Sciences, Belgrade, Serbia

P. Adzic[43], P. Cirkovic, D. Devetak, M. Dordevic, J. Milosevic, V. Rekovic

Centro de Investigaciones Energéticas Medioambientales y Tecnológicas (CIEMAT), Madrid, Spain

J. Alcaraz Maestre, M. Barrio Luna, E. Calvo, M. Cerrada, M. Chamizo Llatas, N. Colino, B. De La Cruz, A. Delgado Peris, A. Escalante Del Valle, C. Fernandez Bedoya, J.P. Fernández Ramos, J. Flix, M.C. Fouz, P. Garcia-Abia, O. Gonzalez Lopez, S. Goy Lopez, J.M. Hernandez, M.I. Josa, E. Navarro De Martino, A. Pérez-Calero Yzquierdo, J. Puerta Pelayo, A. Quintario Olmeda, I. Redondo, L. Romero, M.S. Soares

Universidad Autónoma de Madrid, Madrid, Spain

J.F. de Trocóniz, M. Missiroli, D. Moran

Universidad de Oviedo, Oviedo, Spain

J. Cuevas, J. Fernandez Menendez, I. Gonzalez Caballero, J.R. González Fernández, E. Palencia Cortezon, S. Sanchez Cruz, I. Suárez Andrés, J.M. Vizan Garcia

Instituto de Física de Cantabria (IFCA), CSIC-Universidad de Cantabria, Santander, Spain

I.J. Cabrillo, A. Calderon, J.R. Castiñeiras De Saa, E. Curras, M. Fernandez, J. Garcia-Ferrero, G. Gomez, A. Lopez Virto, J. Marco, C. Martinez Rivero, F. Matorras, J. Piedra Gomez, T. Rodrigo, A. Ruiz-Jimeno, L. Scodellaro, N. Trevisani, I. Vila, R. Vilar Cortabitarte

CERN, European Organization for Nuclear Research, Geneva, Switzerland

D. Abbaneo, E. Auffray, G. Auzinger, M. Bachtis, P. Baillon, A.H. Ball, D. Barney, P. Bloch, A. Bocci, A. Bonato, C. Botta, T. Camporesi, R. Castello, M. Cepeda, G. Cerminara, M. D'Alfonso, D. d'Enterria, A. Dabrowski, V. Daponte, A. David, M. De Gruttola, F. De Guio, A. De Roeck, E. Di Marco[44], M. Dobson, B. Dorney, T. du Pree, D. Duggan, M. Dünser, N. Dupont, A. Elliott-Peisert, S. Fartoukh, G. Franzoni, J. Fulcher, W. Funk, D. Gigi, K. Gill, M. Girone, F. Glege, D. Gulhan, S. Gundacker, M. Guthoff, J. Hammer, P. Harris, J. Hegeman, V. Innocente, P. Janot, H. Kirschenmann, V. Knünz, A. Kornmayer[15], M.J. Kortelainen, K. Kousouris, M. Krammer[1], P. Lecoq, C. Lourenço, M.T. Lucchini, L. Malgeri, M. Mannelli, A. Martelli, F. Meijers, S. Mersi, E. Meschi, F. Moortgat, S. Morovic, M. Mulders, H. Neugebauer, S. Orfanelli, L. Orsini, L. Pape, E. Perez, M. Peruzzi, A. Petrilli, G. Petrucciani, A. Pfeiffer, M. Pierini, A. Racz, T. Reis, G. Rolandi[45], M. Rovere, M. Ruan, H. Sakulin, J.B. Sauvan, C. Schäfer, C. Schwick, M. Seidel, A. Sharma, P. Silva, M. Simon, P. Sphicas[46], J. Steggemann, M. Stoye, Y. Takahashi, M. Tosi, D. Treille, A. Triossi, A. Tsirou, V. Veckalns[47], G.I. Veres[21], N. Wardle, A. Zagozdzinska[35], W.D. Zeuner

Paul Scherrer Institut, Villigen, Switzerland

W. Bertl, K. Deiters, W. Erdmann, R. Horisberger, Q. Ingram, H.C. Kaestli, D. Kotlinski, U. Langenegger, T. Rohe

Institute for Particle Physics, ETH Zurich, Zurich, Switzerland

F. Bachmair, L. Bäni, L. Bianchini, B. Casal, G. Dissertori, M. Dittmar, M. Donegà, P. Eller, C. Grab, C. Heidegger, D. Hits, J. Hoss, G. Kasieczka, P. Lecomte[†], W. Lustermann, B. Mangano, M. Marionneau, P. Martinez Ruiz del Arbol, M. Masciovecchio, M.T. Meinhard, D. Meister, F. Micheli, P. Musella, F. Nessi-Tedaldi, F. Pandolfi, J. Pata, F. Pauss, G. Perrin, L. Perrozzi, M. Quittnat, M. Rossini, M. Schönenberger, A. Starodumov[48], V.R. Tavolaro, K. Theofilatos, R. Wallny

Universität Zürich, Zurich, Switzerland

T.K. Aarrestad, C. Amsler[49], L. Caminada, M.F. Canelli, A. De Cosa, C. Galloni, A. Hinzmann, T. Hreus, B. Kilminster, C. Lange, J. Ngadiuba, D. Pinna, G. Rauco, P. Robmann, D. Salerno, Y. Yang

National Central University, Chung-Li, Taiwan

V. Candelise, T.H. Doan, Sh. Jain, R. Khurana, M. Konyushikhin, C.M. Kuo, W. Lin, Y.J. Lu, A. Pozdnyakov, S.S. Yu

National Taiwan University (NTU), Taipei, Taiwan

Arun Kumar, P. Chang, Y.H. Chang, Y.W. Chang, Y. Chao, K.F. Chen, P.H. Chen, C. Dietz, F. Fiori, W.-S. Hou, Y. Hsiung, Y.F. Liu, R.-S. Lu, M. Miñano Moya, E. Paganis, A. Psallidas, J.f. Tsai, Y.M. Tzeng

Chulalongkorn University, Faculty of Science, Department of Physics, Bangkok, Thailand

B. Asavapibhop, G. Singh, N. Srimanobhas, N. Suwonjandee

Cukurova University - Physics Department, Science and Art Faculty

M.N. Bakirci[50], S. Damarseckin, Z.S. Demiroglu, C. Dozen, E. Eskut, S. Girgis, G. Gokbulut, Y. Guler, E. Gurpinar, I. Hos, E.E. Kangal[51], O. Kara, U. Kiminsu, M. Oglakci, G. Onengut[52], K. Ozdemir[53], S. Ozturk[50], A. Polatoz, D. Sunar Cerci[54], S. Turkcapar, I.S. Zorbakir, C. Zorbilmez

Middle East Technical University, Physics Department, Ankara, Turkey

B. Bilin, S. Bilmis, B. Isildak[55], G. Karapinar[56], M. Yalvac, M. Zeyrek

Bogazici University, Istanbul, Turkey

E. Gülmez, M. Kaya[57], O. Kaya[58], E.A. Yetkin[59], T. Yetkin[60]

Istanbul Technical University, Istanbul, Turkey

A. Cakir, K. Cankocak, S. Sen[61]

Institute for Scintillation Materials of National Academy of Science of Ukraine, Kharkov, Ukraine

B. Grynyov

National Scientific Center, Kharkov Institute of Physics and Technology, Kharkov, Ukraine

L. Levchuk, P. Sorokin

University of Bristol, Bristol, United Kingdom

R. Aggleton, F. Ball, L. Beck, J.J. Brooke, D. Burns, E. Clement, D. Cussans, H. Flacher, J. Goldstein, M. Grimes, G.P. Heath, H.F. Heath, J. Jacob, L. Kreczko, C. Lucas, D.M. Newbold[62], S. Paramesvaran, A. Poll, T. Sakuma, S. Seif El Nasr-storey, D. Smith, V.J. Smith

Rutherford Appleton Laboratory, Didcot, United Kingdom

D. Barducci, K.W. Bell, A. Belyaev[63], C. Brew, R.M. Brown, L. Calligaris, D. Cieri, D.J.A. Cockerill, J.A. Coughlan, K. Harder, S. Harper, E. Olaiya, D. Petyt, C.H. Shepherd-Themistocleous, A. Thea, I.R. Tomalin, T. Williams

Imperial College, London, United Kingdom

M. Baber, R. Bainbridge, O. Buchmuller, A. Bundock, D. Burton, S. Casasso, M. Citron, D. Colling, L. Corpe, P. Dauncey, G. Davies, A. De Wit, M. Della Negra, R. Di Maria, P. Dunne, A. Elwood, D. Futyan, Y. Haddad, G. Hall, G. Iles, T. James, R. Lane, C. Laner, R. Lucas[62], L. Lyons, A.-M. Magnan, S. Malik, L. Mastrolorenzo, J. Nash,

A. Nikitenko[48], J. Pela, B. Penning, M. Pesaresi, D.M. Raymond, A. Richards, A. Rose, C. Seez, S. Summers, A. Tapper, K. Uchida, M. Vazquez Acosta[64], T. Virdee[15], J. Wright, S.C. Zenz

Brunel University, Uxbridge, United Kingdom

J.E. Cole, P.R. Hobson, A. Khan, P. Kyberd, D. Leslie, I.D. Reid, P. Symonds, L. Teodorescu, M. Turner

Baylor University, Waco, U.S.A.

A. Borzou, K. Call, J. Dittmann, K. Hatakeyama, H. Liu, N. Pastika

The University of Alabama, Tuscaloosa, U.S.A.

O. Charaf, S.I. Cooper, C. Henderson, P. Rumerio

Boston University, Boston, U.S.A.

D. Arcaro, A. Avetisyan, T. Bose, D. Gastler, D. Rankin, C. Richardson, J. Rohlf, L. Sulak, D. Zou

Brown University, Providence, U.S.A.

G. Benelli, E. Berry, D. Cutts, A. Garabedian, J. Hakala, U. Heintz, J.M. Hogan, O. Jesus, E. Laird, G. Landsberg, Z. Mao, M. Narain, S. Piperov, S. Sagir, E. Spencer, R. Syarif

University of California, Davis, Davis, U.S.A.

R. Breedon, G. Breto, D. Burns, M. Calderon De La Barca Sanchez, S. Chauhan, M. Chertok, J. Conway, R. Conway, P.T. Cox, R. Erbacher, C. Flores, G. Funk, M. Gardner, W. Ko, R. Lander, C. Mclean, M. Mulhearn, D. Pellett, J. Pilot, F. Ricci-Tam, S. Shalhout, J. Smith, M. Squires, D. Stolp, M. Tripathi, S. Wilbur, R. Yohay

University of California, Los Angeles, U.S.A.

R. Cousins, P. Everaerts, A. Florent, J. Hauser, M. Ignatenko, D. Saltzberg, E. Takasugi, V. Valuev, M. Weber

University of California, Riverside, Riverside, U.S.A.

K. Burt, R. Clare, J. Ellison, J.W. Gary, G. Hanson, J. Heilman, P. Jandir, E. Kennedy, F. Lacroix, O.R. Long, M. Olmedo Negrete, M.I. Paneva, A. Shrinivas, H. Wei, S. Wimpenny, B. R. Yates

University of California, San Diego, La Jolla, U.S.A.

J.G. Branson, G.B. Cerati, S. Cittolin, M. Derdzinski, R. Gerosa, A. Holzner, D. Klein, V. Krutelyov, J. Letts, I. Macneill, D. Olivito, S. Padhi, M. Pieri, M. Sani, V. Sharma, S. Simon, M. Tadel, A. Vartak, S. Wasserbaech[65], C. Welke, J. Wood, F. Würthwein, A. Yagil, G. Zevi Della Porta

University of California, Santa Barbara - Department of Physics, Santa Barbara, U.S.A.

R. Bhandari, J. Bradmiller-Feld, C. Campagnari, A. Dishaw, V. Dutta, K. Flowers, M. Franco Sevilla, P. Geffert, C. George, F. Golf, L. Gouskos, J. Gran, R. Heller, J. Incandela, N. Mccoll, S.D. Mullin, A. Ovcharova, J. Richman, D. Stuart, I. Suarez, C. West, J. Yoo

California Institute of Technology, Pasadena, U.S.A.

D. Anderson, A. Apresyan, J. Bendavid, A. Bornheim, J. Bunn, Y. Chen, J. Duarte, J.M. Lawhorn, A. Mott, H.B. Newman, C. Pena, M. Spiropulu, J.R. Vlimant, S. Xie, R.Y. Zhu

Carnegie Mellon University, Pittsburgh, U.S.A.

M.B. Andrews, V. Azzolini, T. Ferguson, M. Paulini, J. Russ, M. Sun, H. Vogel, I. Vorobiev

University of Colorado Boulder, Boulder, U.S.A.

J.P. Cumalat, W.T. Ford, F. Jensen, A. Johnson, M. Krohn, T. Mulholland, K. Stenson, S.R. Wagner

Cornell University, Ithaca, U.S.A.

J. Alexander, J. Chaves, J. Chu, S. Dittmer, K. Mcdermott, N. Mirman, G. Nicolas Kaufman, J.R. Patterson, A. Rinkevicius, A. Ryd, L. Skinnari, L. Soffi, S.M. Tan, Z. Tao, J. Thom, J. Tucker, P. Wittich, M. Zientek

Fairfield University, Fairfield, U.S.A.

D. Winn

Fermi National Accelerator Laboratory, Batavia, U.S.A.

S. Abdullin, M. Albrow, G. Apollinari, S. Banerjee, L.A.T. Bauerdick, A. Beretvas, J. Berryhill, P.C. Bhat, G. Bolla, K. Burkett, J.N. Butler, H.W.K. Cheung, F. Chlebana, S. Cihangir[†], M. Cremonesi, V.D. Elvira, I. Fisk, J. Freeman, E. Gottschalk, L. Gray, D. Green, S. Grünendahl, O. Gutsche, D. Hare, R.M. Harris, S. Hasegawa, J. Hirschauer, Z. Hu, B. Jayatilaka, S. Jindariani, M. Johnson, U. Joshi, B. Klima, B. Kreis, S. Lammel, J. Linacre, D. Lincoln, R. Lipton, T. Liu, R. Lopes De Sá, J. Lykken, K. Maeshima, N. Magini, J.M. Marraffino, S. Maruyama, D. Mason, P. McBride, P. Merkel, S. Mrenna, S. Nahn, C. Newman-Holmes[†], V. O'Dell, K. Pedro, O. Prokofyev, G. Rakness, L. Ristori, E. Sexton-Kennedy, A. Soha, W.J. Spalding, L. Spiegel, S. Stoynev, N. Strobbe, L. Taylor, S. Tkaczyk, N.V. Tran, L. Uplegger, E.W. Vaandering, C. Vernieri, M. Verzocchi, R. Vidal, M. Wang, H.A. Weber, A. Whitbeck

University of Florida, Gainesville, U.S.A.

D. Acosta, P. Avery, P. Bortignon, D. Bourilkov, A. Brinkerhoff, A. Carnes, M. Carver, D. Curry, S. Das, R.D. Field, I.K. Furic, J. Konigsberg, A. Korytov, P. Ma, K. Matchev, H. Mei, P. Milenovic[66], G. Mitselmakher, D. Rank, L. Shchutska, D. Sperka, L. Thomas, J. Wang, S. Wang, J. Yelton

Florida International University, Miami, U.S.A.

S. Linn, P. Markowitz, G. Martinez, J.L. Rodriguez

Florida State University, Tallahassee, U.S.A.

A. Ackert, J.R. Adams, T. Adams, A. Askew, S. Bein, B. Diamond, S. Hagopian, V. Hagopian, K.F. Johnson, A. Khatiwada, H. Prosper, A. Santra, M. Weinberg

Florida Institute of Technology, Melbourne, U.S.A.

M.M. Baarmand, V. Bhopatkar, S. Colafranceschi[67], M. Hohlmann, D. Noonan, T. Roy, F. Yumiceva

University of Illinois at Chicago (UIC), Chicago, U.S.A.

M.R. Adams, L. Apanasevich, D. Berry, R.R. Betts, I. Bucinskaite, R. Cavanaugh, O. Evdokimov, L. Gauthier, C.E. Gerber, D.J. Hofman, P. Kurt, C. O'Brien, I.D. Sandoval Gonzalez, P. Turner, N. Varelas, H. Wang, Z. Wu, M. Zakaria, J. Zhang

The University of Iowa, Iowa City, U.S.A.

B. Bilki[68], W. Clarida, K. Dilsiz, S. Durgut, R.P. Gandrajula, M. Haytmyradov, V. Khristenko, J.-P. Merlo, H. Mermerkaya[69], A. Mestvirishvili, A. Moeller, J. Nachtman, H. Ogul, Y. Onel, F. Ozok[70], A. Penzo, C. Snyder, E. Tiras, J. Wetzel, K. Yi

Johns Hopkins University, Baltimore, U.S.A.

I. Anderson, B. Blumenfeld, A. Cocoros, N. Eminizer, D. Fehling, L. Feng, A.V. Gritsan, P. Maksimovic, M. Osherson, J. Roskes, U. Sarica, M. Swartz, M. Xiao, Y. Xin, C. You

The University of Kansas, Lawrence, U.S.A.

A. Al-bataineh, P. Baringer, A. Bean, S. Boren, J. Bowen, C. Bruner, J. Castle, L. Forthomme, R.P. Kenny III, A. Kropivnitskaya, D. Majumder, W. Mcbrayer, M. Murray, S. Sanders, R. Stringer, J.D. Tapia Takaki, Q. Wang

Kansas State University, Manhattan, U.S.A.

A. Ivanov, K. Kaadze, S. Khalil, M. Makouski, Y. Maravin, A. Mohammadi, L.K. Saini, N. Skhirtladze, S. Toda

Lawrence Livermore National Laboratory, Livermore, U.S.A.

F. Rebassoo, D. Wright

University of Maryland, College Park, U.S.A.

C. Anelli, A. Baden, O. Baron, A. Belloni, B. Calvert, S.C. Eno, C. Ferraioli, J.A. Gomez, N.J. Hadley, S. Jabeen, R.G. Kellogg, T. Kolberg, J. Kunkle, Y. Lu, A.C. Mignerey, Y.H. Shin, A. Skuja, M.B. Tonjes, S.C. Tonwar

Massachusetts Institute of Technology, Cambridge, U.S.A.

D. Abercrombie, B. Allen, A. Apyan, R. Barbieri, A. Baty, R. Bi, K. Bierwagen, S. Brandt, W. Busza, I.A. Cali, Z. Demiragli, L. Di Matteo, G. Gomez Ceballos, M. Goncharov, D. Hsu, Y. Iiyama, G.M. Innocenti, M. Klute, D. Kovalskyi, K. Krajczar, Y.S. Lai, Y.-J. Lee, A. Levin, P.D. Luckey, A.C. Marini, C. Mcginn, C. Mironov, S. Narayanan, X. Niu, C. Paus, C. Roland, G. Roland, J. Salfeld-Nebgen, G.S.F. Stephans, K. Sumorok, K. Tatar, M. Varma, D. Velicanu, J. Veverka, J. Wang, T.W. Wang, B. Wyslouch, M. Yang, V. Zhukova

University of Minnesota, Minneapolis, U.S.A.

A.C. Benvenuti, R.M. Chatterjee, A. Evans, A. Finkel, A. Gude, P. Hansen, S. Kalafut, S.C. Kao, Y. Kubota, Z. Lesko, J. Mans, S. Nourbakhsh, N. Ruckstuhl, R. Rusack, N. Tambe, J. Turkewitz

University of Mississippi, Oxford, U.S.A.

J.G. Acosta, S. Oliveros

University of Nebraska-Lincoln, Lincoln, U.S.A.

E. Avdeeva, R. Bartek, K. Bloom, D.R. Claes, A. Dominguez, C. Fangmeier, R. Gonzalez Suarez, R. Kamalieddin, I. Kravchenko, A. Malta Rodrigues, F. Meier, J. Monroy, J.E. Siado, G.R. Snow, B. Stieger

State University of New York at Buffalo, Buffalo, U.S.A.

M. Alyari, J. Dolen, J. George, A. Godshalk, C. Harrington, I. Iashvili, J. Kaisen, A. Kharchilava, A. Kumar, A. Parker, S. Rappoccio, B. Roozbahani

Northeastern University, Boston, U.S.A.

G. Alverson, E. Barberis, D. Baumgartel, A. Hortiangtham, B. Knapp, A. Massironi, D.M. Morse, D. Nash, T. Orimoto, R. Teixeira De Lima, D. Trocino, R.-J. Wang, D. Wood

Northwestern University, Evanston, U.S.A.

S. Bhattacharya, K.A. Hahn, A. Kubik, A. Kumar, J.F. Low, N. Mucia, N. Odell, B. Pollack, M.H. Schmitt, K. Sung, M. Trovato, M. Velasco

University of Notre Dame, Notre Dame, U.S.A.

N. Dev, M. Hildreth, K. Hurtado Anampa, C. Jessop, D.J. Karmgard, N. Kellams, K. Lannon, N. Marinelli, F. Meng, C. Mueller, Y. Musienko[36], M. Planer, A. Reinsvold, R. Ruchti, G. Smith, S. Taroni, M. Wayne, M. Wolf, A. Woodard

The Ohio State University, Columbus, U.S.A.

J. Alimena, L. Antonelli, J. Brinson, B. Bylsma, L.S. Durkin, S. Flowers, B. Francis, A. Hart, C. Hill, R. Hughes, W. Ji, B. Liu, W. Luo, D. Puigh, B.L. Winer, H.W. Wulsin

Princeton University, Princeton, U.S.A.

S. Cooperstein, O. Driga, P. Elmer, J. Hardenbrook, P. Hebda, D. Lange, J. Luo, D. Marlow, T. Medvedeva, K. Mei, M. Mooney, J. Olsen, C. Palmer, P. Piroué, D. Stickland, C. Tully, A. Zuranski

University of Puerto Rico, Mayaguez, U.S.A.

S. Malik

Purdue University, West Lafayette, U.S.A.

A. Barker, V.E. Barnes, S. Folgueras, L. Gutay, M.K. Jha, M. Jones, A.W. Jung, K. Jung, D.H. Miller, N. Neumeister, X. Shi, J. Sun, A. Svyatkovskiy, F. Wang, W. Xie, L. Xu

Purdue University Calumet, Hammond, U.S.A.

N. Parashar, J. Stupak

Rice University, Houston, U.S.A.

A. Adair, B. Akgun, Z. Chen, K.M. Ecklund, F.J.M. Geurts, M. Guilbaud, W. Li, B. Michlin, M. Northup, B.P. Padley, R. Redjimi, J. Roberts, J. Rorie, Z. Tu, J. Zabel

University of Rochester, Rochester, U.S.A.

B. Betchart, A. Bodek, P. de Barbaro, R. Demina, Y.t. Duh, T. Ferbel, M. Galanti, A. Garcia-Bellido, J. Han, O. Hindrichs, A. Khukhunaishvili, K.H. Lo, P. Tan, M. Verzetti

Rutgers, The State University of New Jersey, Piscataway, U.S.A.

J.P. Chou, E. Contreras-Campana, Y. Gershtein, T.A. Gómez Espinosa, E. Halkiadakis, M. Heindl, D. Hidas, E. Hughes, S. Kaplan, R. Kunnawalkam Elayavalli, S. Kyriacou, A. Lath, K. Nash, H. Saka, S. Salur, S. Schnetzer, D. Sheffield, S. Somalwar, R. Stone, S. Thomas, P. Thomassen, M. Walker

University of Tennessee, Knoxville, U.S.A.

M. Foerster, J. Heideman, G. Riley, K. Rose, S. Spanier, K. Thapa

Texas A&M University, College Station, U.S.A.

O. Bouhali[71], A. Celik, M. Dalchenko, M. De Mattia, A. Delgado, S. Dildick, R. Eusebi, J. Gilmore, T. Huang, E. Juska, T. Kamon[72], R. Mueller, Y. Pakhotin, R. Patel, A. Perloff, L. Perniè, D. Rathjens, A. Rose, A. Safonov, A. Tatarinov, K.A. Ulmer

Texas Tech University, Lubbock, U.S.A.

N. Akchurin, C. Cowden, J. Damgov, C. Dragoiu, P.R. Dudero, J. Faulkner, S. Kunori, K. Lamichhane, S.W. Lee, T. Libeiro, S. Undleeb, I. Volobouev, Z. Wang

Vanderbilt University, Nashville, U.S.A.

A.G. Delannoy, S. Greene, A. Gurrola, R. Janjam, W. Johns, C. Maguire, A. Melo, H. Ni, P. Sheldon, S. Tuo, J. Velkovska, Q. Xu

University of Virginia, Charlottesville, U.S.A.

M.W. Arenton, P. Barria, B. Cox, J. Goodell, R. Hirosky, A. Ledovskoy, H. Li, C. Neu, T. Sinthuprasith, Y. Wang, E. Wolfe, F. Xia

Wayne State University, Detroit, U.S.A.

C. Clarke, R. Harr, P.E. Karchin, P. Lamichhane, J. Sturdy

University of Wisconsin - Madison, Madison, WI, U.S.A.

D.A. Belknap, S. Dasu, L. Dodd, S. Duric, B. Gomber, M. Grothe, M. Herndon, A. Hervé, P. Klabbers, A. Lanaro, A. Levine, K. Long, R. Loveless, I. Ojalvo, T. Perry, G.A. Pierro, G. Polese, T. Ruggles, A. Savin, A. Sharma, N. Smith, W.H. Smith, D. Taylor, N. Woods

†: Deceased
1: Also at Vienna University of Technology, Vienna, Austria
2: Also at State Key Laboratory of Nuclear Physics and Technology, Peking University, Beijing, China
3: Also at Institut Pluridisciplinaire Hubert Curien (IPHC), Université de Strasbourg, CNRS/IN2P3, Strasbourg, France
4: Also at Universidade Estadual de Campinas, Campinas, Brazil
5: Also at Universidade Federal de Pelotas, Pelotas, Brazil
6: Also at Université Libre de Bruxelles, Bruxelles, Belgium
7: Also at Deutsches Elektronen-Synchrotron, Hamburg, Germany

8: Also at Joint Institute for Nuclear Research, Dubna, Russia

9: Also at Helwan University, Cairo, Egypt

10: Now at Zewail City of Science and Technology, Zewail, Egypt

11: Now at Fayoum University, El-Fayoum, Egypt

12: Also at British University in Egypt, Cairo, Egypt

13: Now at Ain Shams University, Cairo, Egypt

14: Also at Université de Haute Alsace, Mulhouse, France

15: Also at CERN, European Organization for Nuclear Research, Geneva, Switzerland

16: Also at Skobeltsyn Institute of Nuclear Physics, Lomonosov Moscow State University, Moscow, Russia

17: Also at RWTH Aachen University, III. Physikalisches Institut A, Aachen, Germany

18: Also at University of Hamburg, Hamburg, Germany

19: Also at Brandenburg University of Technology, Cottbus, Germany

20: Also at Institute of Nuclear Research ATOMKI, Debrecen, Hungary

21: Also at MTA-ELTE Lendület CMS Particle and Nuclear Physics Group, Eötvös Loránd University, Budapest, Hungary

22: Also at Institute of Physics, University of Debrecen, Debrecen, Hungary

23: Also at Indian Institute of Science Education and Research, Bhopal, India

24: Also at Institute of Physics, Bhubaneswar, India

25: Also at University of Visva-Bharati, Santiniketan, India

26: Also at University of Ruhuna, Matara, Sri Lanka

27: Also at Isfahan University of Technology, Isfahan, Iran

28: Also at University of Tehran, Department of Engineering Science, Tehran, Iran

29: Also at Plasma Physics Research Center, Science and Research Branch, Islamic Azad University, Tehran, Iran

30: Also at Università degli Studi di Siena, Siena, Italy

31: Also at Purdue University, West Lafayette, U.S.A.

32: Also at International Islamic University of Malaysia, Kuala Lumpur, Malaysia

33: Also at Malaysian Nuclear Agency, MOSTI, Kajang, Malaysia

34: Also at Consejo Nacional de Ciencia y Tecnología, Mexico city, Mexico

35: Also at Warsaw University of Technology, Institute of Electronic Systems, Warsaw, Poland

36: Also at Institute for Nuclear Research, Moscow, Russia

37: Now at National Research Nuclear University 'Moscow Engineering Physics Institute' (MEPhI), Moscow, Russia

38: Also at St. Petersburg State Polytechnical University, St. Petersburg, Russia

39: Also at University of Florida, Gainesville, U.S.A.

40: Also at P.N. Lebedev Physical Institute, Moscow, Russia

41: Also at California Institute of Technology, Pasadena, U.S.A.

42: Also at Budker Institute of Nuclear Physics, Novosibirsk, Russia

43: Also at Faculty of Physics, University of Belgrade, Belgrade, Serbia

44: Also at INFN Sezione di Roma; Università di Roma, Roma, Italy

45: Also at Scuola Normale e Sezione dell'INFN, Pisa, Italy

46: Also at National and Kapodistrian University of Athens, Athens, Greece

47: Also at Riga Technical University, Riga, Latvia

48: Also at Institute for Theoretical and Experimental Physics, Moscow, Russia

49: Also at Albert Einstein Center for Fundamental Physics, Bern, Switzerland

50: Also at Gaziosmanpasa University, Tokat, Turkey

51: Also at Mersin University, Mersin, Turkey